# Journal Pre-proof

The structure-based optimization of $\delta$-sultone-fused pyrazoles as selective BuChE inhibitors

Ziwen Zhang, Jingli Min, Mengdie Chen, Xia Jiang, Yingying Xu, Huali Qin, Wenjian Tang

Please cite this article as: Z. Zhang, J. Min, M. Chen, X. Jiang, Y. Xu, H. Qin, W. Tang, The structure-based optimization of $\delta$-sultone-fused pyrazoles as selective BuChE inhibitors, *European Journal of Medicinal Chemistry* (2020), doi: https://doi.org/10.1016/j.ejmech.2020.112273.

This is a PDF file of an article that has undergone enhancements after acceptance, such as the addition of a cover page and metadata, and formatting for readability, but it is not yet the definitive version of record. This version will undergo additional copyediting, typesetting and review before it is published in its final form, but we are providing this version to give early visibility of the article. Please note that, during the production process, errors may be discovered which could affect the content, and all legal disclaimers that apply to the journal pertain.
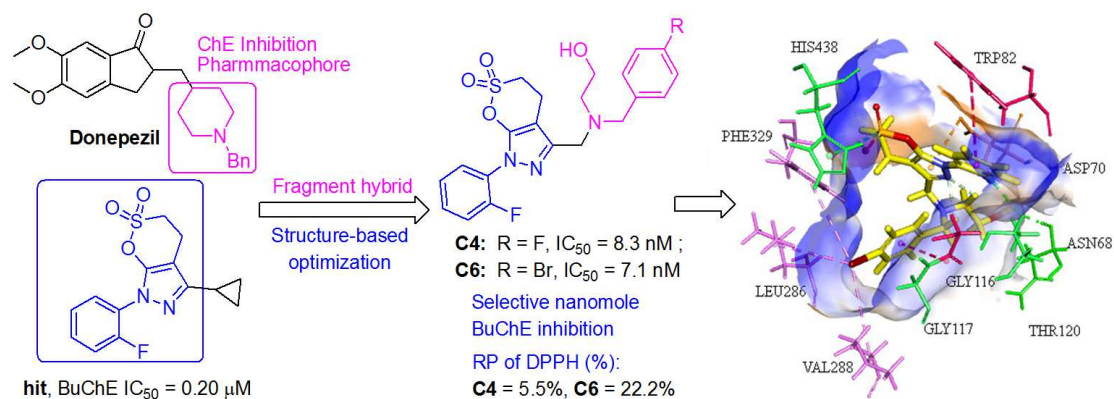
By the introduction of a tertiary benzylamine, structure-based optimization was conducted to significantly improve the potency and selectivity of *δ*-sulfon-fused pyrazole as BuChE inhibitors. Compounds **C4** and **C6** showed high selective nanomolar BuChE inhibitors, mild antioxidant capacity, nontoxicity, lipophilicity and remarkably neuroprotective activity.

# The structure-based optimization of $\delta$-sultone-fused pyrazoles as selective BuChE inhibitors

Ziwen Zhang [a,1], Jingli Min [a,1], Mengdie Chen [a,1], Xia Jiang [a], Yingying Xu [a], Huali Qin [b,*], Wenjian Tang [a,*]

[a] *School of Pharmacy, Anhui Province Key Laboratory of Major Autoimmune Diseases, Anhui Medical University, Hefei 230032, China*
[b] *School of Chemistry, Chemical Engineering and Life Science, Wuhan University of Technology, Wuhan 430070, China*

**Abstract:**

Structure-based optimization was conducted to improve the potency and selectivity of BuChE inhibitors with $\delta$-sulfonolactone-fused pyrazole scaffold. By mimicking the hydrophobic interactions of donepezil at PAS, the introduction of a tertiary benzylamine at 5-position can significantly increase BuChE inhibitory activity. Compounds **C4** and **C6** were identified as high selective nanomolar BuChE inhibitors (IC$_{50}$ = 8.3 and 7.7 nM, respectively), which exhibited mild antioxidant capacity, nontoxicity, lipophilicity and neuroprotective activity. Kinetic studies showed that BuChE inhibition of compound **C6** was mixed-type against BuChE ($K_i$ = 24 nM) and > 2000-fold selectivity for BuChE over AChE. The proposed binding mode of new inhibitors was consistent with the results of structure–activity relationship analysis.

**Keywords:**

Cholinesterase; SuFEx; sultone; pyrazole; structural optimization; Alzheimer's disease

----

*Corresponding author.

E-mail: qinhuali@whut.edu.cn (H.L. Qin); ahmupharm@126.com (W.J. Tang).

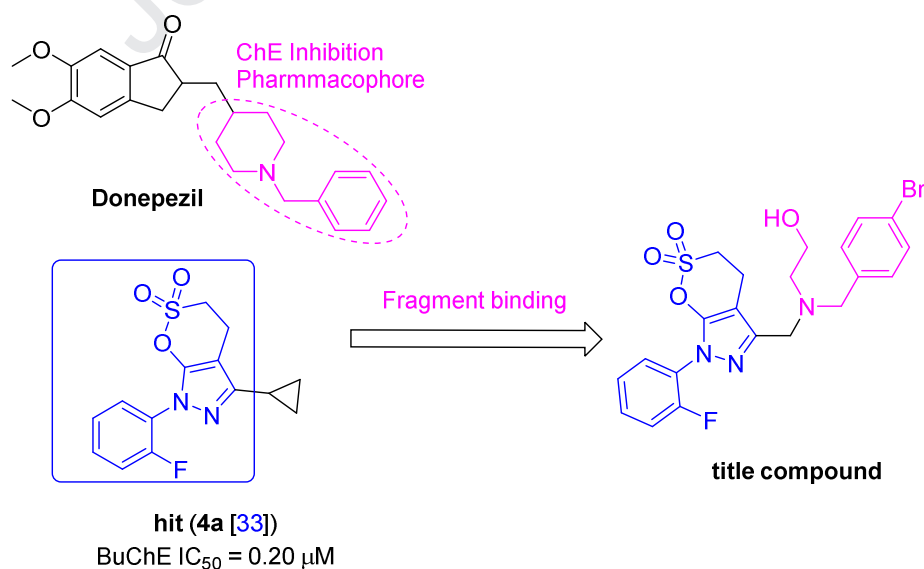[1] Z. Zhang, J. Min and M. Chen contributed equally to this work.

## 1. Introduction

Alzheimer's disease (AD) is a progressive neurodegenerative disorder associated with progressive memory loss and cognitive impairments. Nearly 47 million individuals are affected by Alzheimer's disease in 2018, and 75 million people are affected by 2030 globally [1]. In the past decades, the biological mechanisms on AD widely studied included amyloid plaques of amyloid-β, tau-protein aggregations, cholinergic dysfunction, oxidative stress and biometal dyshomeostasis, et al [2-4]. Up till now, the clinical drugs approved by FDA for AD patients are focused on acetylcholinesterase (AChE) inhibitors such as donepezil, galantamine and rivastigmine. The nebulous and complicated pathogenesis of AD leads to failure of many promising drug candidates, which makes research on AD be still a hot topic [5-8].

Cholinergic system has been extensively studied for the design of anti-AD drugs [9,10]. Physiologically, the activity of ACh in the synapses can be terminated by AChE and butyrylcholinesterase (BuChE). AChE hydrolyzes the majority of ACh in a healthy brain, while, with BuChE in the progressive AD takes over the main role of AChE, reaching almost 80% of the overall ChE activity [11,12]. In the AChE deficient mice, levels of excessive ACh were alleviated by BuChE activity [13,14], moreover in the BuChE-knockout mice, BuChE deficience augmented learning capacities and reduced fibrillar β-amyloid in subcortical structures to lower its toxicity [15-18]. Selective BuChE inhibition might circumvent the classical cholinergic toxicity of AChE inhibitors, therefore, BuChE inhibitors have great potentiality for the treatment of AD, especially the progressive AD [19,20]. Although two ChEs contain a catalytic active site (CAS), a peripheral anionic site (PAS), and a mid-gorge recognition site between CAS and PAS, the wider space of BuChE in acyl-binding site allows larger substrate to be recognized and hydrolyzed [21,22]. The structural features of BuChE help to perform the rational drug design of selective BuChE inhibitors with novel scaffolds [23-26].

The δ-sultone-fused heterocycles can be efficiently synthesized through sulfur (VI) fluoride exchange (SuFEx), which is a rapid and powerful click chemistry reaction owing to the balanced properties of fluoride bonding to hydrogen and sulfur (VI) [27,28]. SuFEx building blocks provided structurally versatile scaffolds in medicinal chemistry.

[29-32]. Recent, a class of novel δ-sulfonolactone-fused pyrazole scaffold was discovered as highly selective submicromolar BuChE inhibitors [33]. SAR on 7-aryl-4,5-disubstituted δ-sultone-fused pyrazoles showed that (i) C4-, C5-, N7-substituents affected BuChE inhibition, however compounds with $CH_2$ at C4 position showed better BuChE inhibition; (ii) the volume of C5-substituent affected BuChE inhibition; (iii) BuChE inhibition of 2-substituent at N7-phenyl ring was better than that of 3-substituent; (iv) compound **4a** was identified as a most potent BuChE inhibitor ($IC_{50}$ = 0.20 μM). Moreover, this scaffold showed reversible, mixed-type BuChE inhibitory activity, which may be used to improve disease symptoms in progressive AD.

The molecular modeling results showed that the active compound is accommodated into hBuChE *via* π−S interaction and hydrophobic interactions, and its δ-sultone ring falls into the hydrolysis sub-pocket of hBuChE active site, however, it is not observed for the interaction between the δ-sultone-fused pyrazole scaffold and PAS of BuChE. Generally, a ChE inhibitor (reversible or pseudo-irreversible) contains a basic nitrogen atom crucial for the interaction with the ChE binding site. Therefore, the inhibitors were designed for optimal binding to BuChE, and targeting was confirmed through docking analysis [34,35]. Herein, we report the structure-based optimization, synthesis, and evaluation for their ChE inhibition to further improve the potency and selectivity of this series of BuChE inhibitors (Fig. 1).



Donepezil

ChE Inhibition Pharmmacophore

Fragment binding

title compound

hit (**4a** [33])
BuChE $IC_{50}$ = 0.20 μM

**Fig. 1**. The design strategy of structural optimization in this study.

## 2. Results and Discussion

### 2.1. Chemistry

According to our recent work, $\delta$-sultone-fused pyrazoles as the lead scaffold was used to synthesize the following compounds (series **A–D**).

Firstly, to know that C5-/N7-substituents of $\delta$-sultone-fused pyrazoles affected BuChE inhibition, series **A** were synthesized as shown in Scheme 1 through the direct annulation of ethenesulfonyl fluoride (ESF) under equimolar amounts of pyrazolones and NaHCO$_3$ and 5 mol% DBU in DCM at room temperature for 12 h with good yields.

Secondly, to introduce a basic tertiary amine group, ethyl chloroacetoacetate was used to synthesize the intermediate **5** in dioxane rather than ethanol by condensation reaction. The key intermediate **6** was efficiently synthesized through Sulfur(VI) Fluoride Exchange (SuFEx), and was substituted by a secondary amine to give series **B** and **C** as shown in Scheme 2.

Finally, compounds containing different substituent of the benzylamine at 5-positon were prepared to further study the SAR between the tertiary amine group and BuChE inhibition, for example series **C** and **D** as shown in Scheme 2.
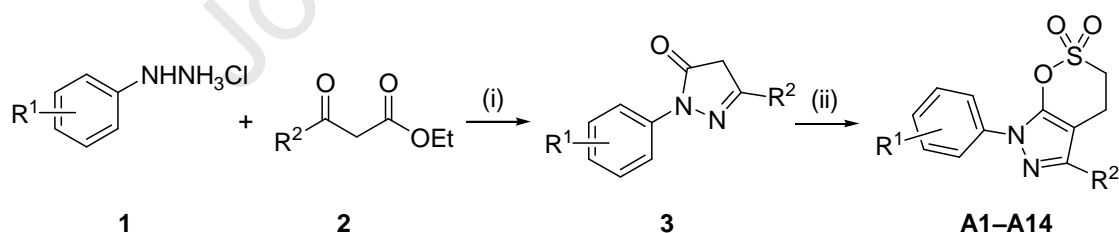


**Scheme 1.** Synthesis of compounds Series **A1–A14**

**Reaction conditions and reagents:** (i) EtOH, AcOH, NaHCO$_3$, reflux, 1.5 h; (ii) ESF (1.0 equiv.), DBU (30 mol%), CH$_2$Cl$_2$, 12 h, r.t.
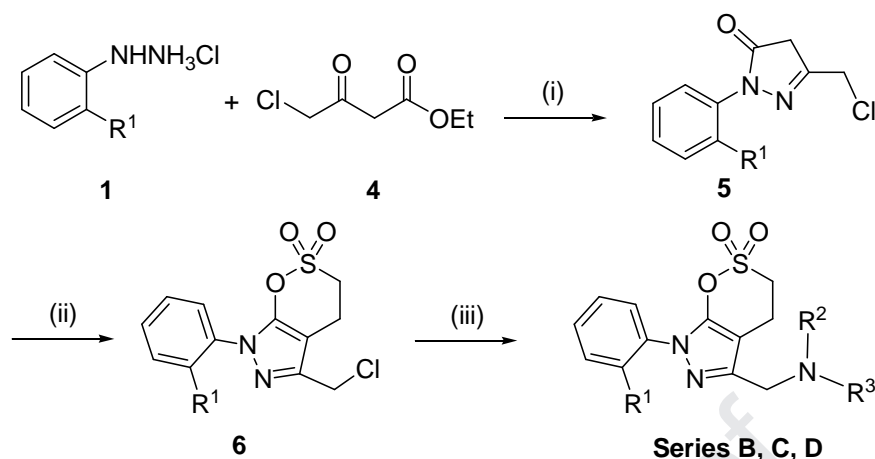
**Scheme 2.** Synthesis of compounds Series **B1–B14**, **C1–C10** and **D1–D10** (for the intermediate **6**, **B1**: $R^1$ = Cl; **B8**: $R^1$ = F)

**Reaction conditions and reagents:** (i) dioxane, 60ºC, 12 h; (ii) ESF (1.0 equiv.), DBU (30 mol%), $CH_2Cl_2$, 12 h, r.t.; (iii) $HNR^2R^3$, $CH_3CN$, $K_2CO_3$, r.t.

*2.2. Inhibition of Equine BuChE and Electrophorus electricus AChE*

The $\delta$-sulfonolactone-fused pyrazoles were evaluated for their activity with equine BuChE (eqBuChE) and *Electrophorus electricus* AChE (EeAChE), using modified Ellman's method.

**Table 1**. **ChE inhibitory activity of compounds A1–A14.** [a]



| Compd. | $R^1$ | $R^2$ | IC$_{50}$, µM (or inhibition% at 20 µM) | |
|--------|-------|-------|---------------------------|-------------------|
| | | | AChE [b] | BuChE [c] |
| **A1** | 2-F | Me | *na* [d] | 1.19±0.47 |
| **A2** | 2-Cl | cyclopropyl | *na* [d] | 0.18±0.01 |

| A3 | 3-Cl | cyclopropyl | *na* [d] | 0.70±0.34 |
| A4 | 2-F | cyclopropyl | *na* [d] | 0.14±0.02 |
| A5 | 3-F | cyclopropyl | *na* [d] | 0.37±0.09 |
| A6 | 2-F | phenyl | *na* [d] | 0.18±0.04 |
| A7 | 2-F | 4-Cl-phenyl | *na* [d] | 0.20±0.05 |
| A8 | 2-F | 4-Br-phenyl | *na* [d] | 0.47±0.24 |
| A9 | 2-F | 4-F-phenyl | *na* [d] | 0.16±0.04 |
| A10 | 2-Cl | phenyl | *na* [d] | 0.17±0.03 |
| A11 | 2-Cl | 4-Cl-phenyl | *na* [d] | 1.58±0.38 |
| A12 | 2-Cl | 4-Br-phenyl | *na* [d] | 3.69±2.90 |
| A13 | 2-Cl | 4-F-phenyl | *na* [d] | 0.13±0.07 |
| A14 | 3-Cl | 4-MeO-phenyl | *na* [d] | 8.78±0.52 |

[a] Each $IC_{50}$ value is the mean ± SEM from at least three independent experiments.

[b] AChE from electric eel. *na*, no inhibitory activity (%) against EeAChE at 20 µM.

[c] BuChE from horse serum. Positive control compounds had the following results (compound: EeAChE $IC_{50}$, eqBuChE $IC_{50}$): donepezil: 0.025 µM, 10.38 µM; rivastigmine: > 20 µM, 0.56 µM.
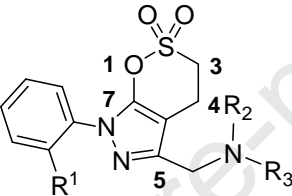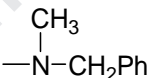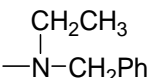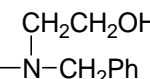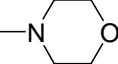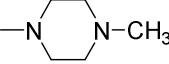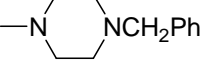
[d] *na* = no inhibitory activity
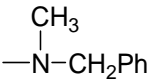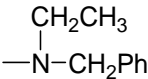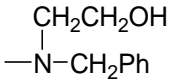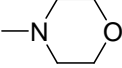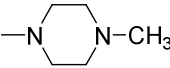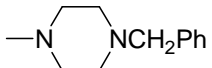
As shown in Table 1, compounds **A1–A10** and **A13** (series **A**) exhibited the submicromolar inhibitory effect on BuChE ($IC_{50}$ values: 0.1–0.7 µM). Compounds with 2-substituent at $R^1$ position showed better BuChE inhibition than those with the corresponding 4-/3-substituent (**A2** > **A3**; **A4** > **A5**). For the 2-substituted group of N7-benzene ring, the activity of 2-F substituent is superior to that of 2-Cl substituent (**A4** > **A2**; **A7** > **A11**; **A8** > **A12**; **A9** > **A13;** except for **A10** ≈ **A6**). Moreover, for the

substituent on the benzene ring at $R^2$ position, the order of BuChE inhibitory activity is 4-F > H > 4-Cl > 4-Br (for example, **A9** > **A6** > **A7** > **A8** for $R^1$ = 2-F; **A13** > **A10** > **A11** > **A12** for $R^1$ = 2-Cl). Based on the above SAR analysis, it was obvious that compounds with 2-F or 2-Cl at $R^1$ position exhibited better BuChE inhibitory activity. Due to a basic group being important for ChE inhibitor, the introduction of a tertiary amine at $R^2$ position may improve the BuChE inhibitory activity. Therefore, series **B** were synthesized and evaluated for their ChE activity.

**Table 2**. ChE inhibitory activity of compounds B1–B14. [a]



| Compd. | $R^1$ | $NR^2R^3$ | IC$_{50}$, μM (or inhibition % at 20 μM) | |
| --- | --- | --- | --- | --- |
| | | | AChE [b] | BuChE [c] |
| **B1** | 2-Cl | —Cl | na [d] | 0.20±0.01 |
| **B2** | 2-Cl | CH$_3$ / —N–CH$_2$Ph | na [d] | 0.07±0.02 |
| **B3** | 2-Cl | CH$_2$CH$_3$ / —N–CH$_2$Ph | na [d] | 0.05±0.02 |
| **B4** | 2-Cl | CH$_2$CH$_2$OH / —N–CH$_2$Ph | na [d] | 0.04±0.02 |
| **B5** | 2-Cl | —N⟩O (morpholine) | na [d] | 0.41±0.10 |
| **B6** | 2-Cl | —N⟩N–CH$_3$ | na [d] | 2.22±0.63 |
| **B7** | 2-Cl | —N⟩NCH$_2$Ph | na [d] | 0.46±0.23 |

| B8 | 2-F | —Cl | na [d] | 0.19±0.15 |
| B9 | 2-F | CH$_3$<br>\|<br>—N−CH$_2$Ph | na [d] | 0.08±0.05 |
| B10 | 2-F | CH$_2$CH$_3$<br>\|<br>—N−CH$_2$Ph | na [d] | 0.08±0.01 |
| B11 | 2-F | CH$_2$CH$_2$OH<br>\|<br>—N−CH$_2$Ph | na [d] | 0.04±0.02 |
| B12 | 2-F | —N◯O | na [d] | 0.15±0.06 |
| B13 | 2-F | —N◯N−CH$_3$ | na [d] | 2.17±1.01 |
| B14 | 2-F | —N◯NCH$_2$Ph | na [d] | 0.68±0.11 |

[a] Each IC$_{50}$ value is the mean ± SEM from at least three independent experiments.

[b] AChE from electric eel. na, no inhibitory activity (%) against EeAChE at 20 μM.

[c] BuChE from horse serum. Positive control compounds had the following results (compound, EeAChE IC$_{50}$, eqBuChE IC$_{50}$): donepezil, 0.025 μM, 10.38 μM; rivastigmine, > 60 μM, 0.56 μM.

[d] na = no inhibitory activity

As shown in Table 2, when both R$^2$ and R$^3$ are aliphatic substituent, the activity isn't improved compared to those of series **A**. The introduction of an aromatic group increased the activity (**B7** > **B6**, **B14** > **B13**). According to the structure characteristics of donepezil, the introduction of a tertiary benzylamine at 5-position can significantly increase BuChE inhibitory activity. Some of δ-sultone-fused pyrazoles (series **B**) exhibited nanomolar inhibition against BuChE. Another substituent of a tertiary benzylamine affected BuChE inhibition, for example, the order of IC$_{50}$ values for BuChE inhibition is hydroxyethyl > ethyl > methyl (**B4** > **B3** > **B2** for R$^1$ = 2-Cl; **B11** > **B10** > **B9** for R$^1$ = 2-F). To further study the relationship between the substituted benzyl and BuChE inhibition, a series of substituted phenyl-methyl derivatives were prepared and evaluated their ChE inhibitory

activity (Table 3).

**Table 3**. **ChE inhibitory activity of compounds C1–C10.** [a]



| Compd. | R$^1$ | IC$_{50}$, μM (or inhibition% at 20 μM) | | RP of DPPH assay [d] |
|---|---|---|---|---|
| | | AChE [b] | BuChE [c] | |
| **C1** | 3-F | na [e] | 0.09±0.08 | 5.0% |
| **C2** | 3-Cl | na [e] | 0.19±0.10 | 4.7% |
| **C3** | 3-Br | na [e] | 0.33±0.17 | 0.8% |
| **C4** | 4-F | na [e] | 0.0083±0.0015 | 5.5% |
| **C5** | 4-Cl | na [e] | 0.09±0.05 | 10.2% |
| **C6** | 4-Br | 43.3±4.7% | 0.0077±0.0006 | 22.2% |
| **C7** | 2,4-Cl | na [e] | 0.09±0.05 | 1.8% |
| **C8** | 4-CH$_3$ | na [e] | 0.17±0.09 | 5.2% |
| **C9** | 4-OCH$_3$ | na [e] | 0.26±0.13 | 3.2% |
| **C10** | 3,4-OCH$_3$ | na [e] | 0.56±0.36 | 5.5% |

[a] Each IC$_{50}$ value is the mean ± SEM from at least three independent experiments.

[b] AChE from electric eel. *na*, no inhibitory activity (%) against EeAChE at 20 μM.
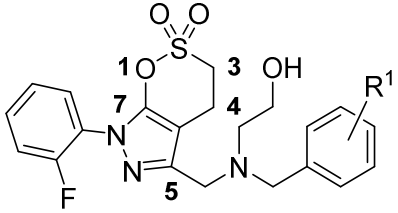
[c] BuChE from horse serum. Positive control compounds had the following results (compound, EeAChE IC$_{50}$, eqBuChE IC$_{50}$): donepezil, 0.025 μM, 10.38 μM; rivastigmine, > 60 μM, 0.56 μM.

[d] RP of 1, 1-Diphenyl-2-picrylhydrazyl (DPPH) (%) = reduction percentage of DPPH,

compounds at a concentration of 100 μM.

[e] *na* = no inhibitory activity

As shown in Table 3, the substituent of benzene ring at 5-positon of scaffold affected the BuChE inhibitory activity: (i) the activity of compounds with 4-halogen substituent is superior to that of compounds with 3-halogen substitution (**C4** > **C1**; **C5** > **C2**; **C6** > **C3**); (ii) compounds with 4-halogen substituent exhibited better BuChE inhibition (**C4** > **C7**, **C5** > **C7**, **C6** > **C7**; **C4** > **C8**, **C5** > **C8**, **C6** > **C8**); (iii) compounds **C4** (4-F) and **C6** (4-Br) had the best BuChE activity (IC$_{50}$ = 8.3 and 7.7 nM, respectively).

**Table 4**. **ChE inhibitory activity of compounds D1–D10.** [a]



| Compd. | R$^1$ | R$^2$ | IC$_{50}$, μM (or inhibition% at 20 μM) | | RP of DPPH assay [d] |
| :---: | :---: | :---: | :---: | :---: | :---: |
| | | | AChE [b] | BuChE [c] | |
| **D1** | -CH$_2$CH$_2$OCH$_3$ | -H | *na* [e] | 0.24±0.12 | 2.3% |
| **D2** | -CH$_2$CH$_2$OCH$_3$ | -F | *na* [e] | 0.11±.09 | 6.3% |
| **D3** | -CH$_2$CH$_2$OCH$_3$ | -Cl | *na* [e] | 0.09±0.04 | 3.6% |
| **D4** | -CH$_2$CH$_2$OCH$_3$ | -Br | *na* [e] | 0.15±0.02 | 4.8% |
| **B11** | -CH$_2$CH$_3$ | -H | *na* [e] | 0.08±0.01 | 5.4% |
| **D5** | -CH$_2$CH$_3$ | -F | *na* [e] | 0.07±0.01 | 0.6% |
| **D6** | -CH$_2$CH$_3$ | -Cl | *na* [e] | 0.04±0.01 | 4.2% |
| **D7** | -CH$_2$CH$_3$ | -Br | *na* [e] | 0.07±0.01 | 12.9% |

| B10 | -CH$_3$ | -H | *na* [e] | 0.08±0.05 | 1.8% |
|------|---------|-----|-----------|-----------|------|
| D8  | -CH$_3$ | -F  | *na* [e]  | 0.04±0.02 | 5.7% |
| D9  | -CH$_3$ | -Cl | *na* [e]  | 0.02±0.01 | 6.1% |
| D10 | -CH$_3$ | -Br | 33.6±14%  | 0.07±0.02 | 0.2% |

[a] Each IC$_{50}$ value is the mean ± SEM from at least three independent experiments.

[b] AChE from electric eel. *na*, no inhibitory activity (%) against EeAChE at 20 µM.

[c] BuChE from horse serum. Positive control compounds had the following results (compound, EeAChE IC$_{50}$, eqBuChE): donepezil, 0.025 µM, 10.38 µM; rivastigmine, > 60 µM, 0.56 µM.
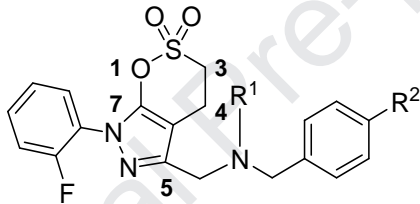
[d] RP of 1,1-Diphenyl-2-picrylhydrazyl (DPPH) (%) = reduction percentage of DPPH, compounds at a concentration of 100 µM.

[e] *na* = no inhibitory activity

The data in Table 4 showed that BuChE inhibition was affected by another substituent (R$^1$) of the benzylamine at 5-positon: (i) the activity significantly decreased when the hydroxyethyl group was methylated (**B11** > **D1**; **C4** > **D2**; **C5** > **D3**; **C6** > **D4**); (ii) compounds **B9**, **B10**, **D5–D10** (R$^1$ = -Me or -Et) with smaller substituent exhibited similar BuChE inhibitory activity (IC$_{50}$ values for 24 – 78 nM). In all in, by simulating the structural characteristics of Donepezil, introduction of a tertiary benzylamine group significantly increased BuChE inhibitory activity of *δ*-sultone-fused pyrazoles to nanomole level.

### 2.3. Molecular docking model of C6 with hBuChE

It has been confirmed that there are two flexible amino acids Leu286 and Val288 in the acyl pocket of hBuChE compared to hAChE. Simultaneously, the two flexible amino acids allows binding of bulkier ligands which may, therefore, be selective for huBuChE [36]. A docking model of hBuChE with compound **C6** (Fig. 2A and 2B) showed that the tertiary benzylamine is extended by a hydroxyethyl chain, and compound **C6** is nicely

bound to hBuChE *via* a strong hydrogen bond interaction between the the hydroxyl unit with Asn68, p–π interaction between the benzyl ring with Leu286, Val288 and Phe329 in the acyl subpocket, and a π–anion interaction between the S atom of sultone ring with His438 in the hydrolysis sub-pocket. In addition, a π–anion interaction is observed between the pyrazole ring at N7 position with Asp70.
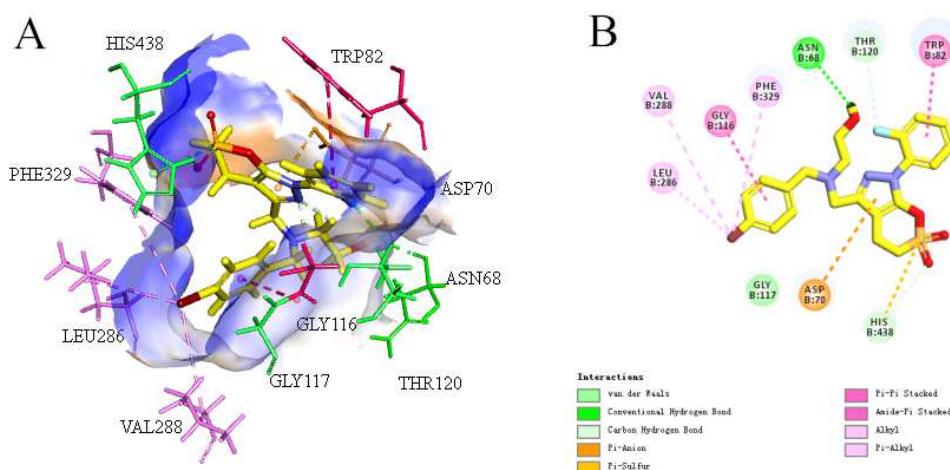


**Fig. 2.** (A) 3D mode of the pocket surface of compound **C6** with receptor hBuChE (PDB ID: 5LKR) performed using Discovery Studio Client v18.1.0. (B) 2D mode of the interaction of compound **C6** with receptor hBuChE (conventional H bond and C–H bond, halogen, π–anion, alkyl, and π–alkyl are represented by green, light green, brown, pink and light pink lines, respectively) performed using Discovery Studio Client v18.1.0.

### 2.4. DPPH radical scavenging activity

1,1-Diphenyl-2-picrylhydrazyl (DPPH) is an extremely effective free radical scavenger that can be used to monitor a chemical reaction that involves free radicals [37,38]. The DPPH assay was performed with ascorbic acid and donepezil as reference antioxidants to evaluate the ability of the synthesized compounds to scavenge activated oxygen species. As shown in Tables 3 and 4, some of the synthesized compounds exhibited mild free radical scavenging activity with the RP of DPPH for 0.2%-22.2% at a concentration of 100 μM, amongst them, compound **C6** showed the best antioxidant

activity, while methylation of ethoxyl group (**D4**) led its activity to decrease.

### 2.5. Kinetic study of eqBuChE inhibition

Compound **C6**, the derivative with the highest inhibitory activity, was subjected to enzyme kinetics analysis to determine the kinetics of BuChE inhibition. As shown in Fig. 3A, the plots of the remaining enzyme activity versus the concentration of enzyme (0, 0.045, 0.090, 0.18, 0.36 and 0.72 U/mL) in the presence of different concentrations of compound **C6** for the catalysis of butyrylcholine gave a series of straight lines. In case of compound **C6** all the lines intersected at the same point. Increasing the inhibitor concentration resulted in a decrease in the slope of the lines, which indicated that compound **C6** were reversible BuChE inhibitors. The slopes and intercepts of the reciprocal Lineweaver–Burk plot presented in Fig. 3B increased with the increase in inhibitor concentration. The intersection of each trend line in the fourth quadrant indicated a mixed-type inhibitory mode. As shown in Fig. 3C, the dissociation constants $K_i$ for compound **C6** from the Lineweavere-Burk secondary plots were estimated to be 24 nM.

Kinetic studies of eqBuChE inhibition Kinetic studies were performed with the same test conditions, using six concentrations of substrate (0.1-1 mM) and four concentrations of inhibitor (0-0.08μM). Apparent inhibition constants and kinetic parameters were calculated within the "Enzyme kinetics" module of Prism 5. The effect of concentrations of compound **C6** on the activity for the catalysis of BuChE at 37ºC was also studied. Assay conditions were same as described in assay protocol except that the final concentration of enzyme was varied (0-0.72 U/mL). Concentrations of compound **C6** (0, 0.02, 0.04, 0.08 μM) were used respectively, for the determination of reversible as well as irreversible binding of inhibitors at enzyme.

**Fig. 3**. Relationship between eqBuChE inhibition and various concentrations of compound **C6** (A). Lineweaver-Burk plots of eqBuChE inhibition kinetics of compound **C6** (B). The Lineweaver-Burk secondary plots of compound **C6** (C). Reciprocals of enzyme activity (eqBuChE) vs reciprocals of substrate (butyrylthiocholine iodide) with different concentrations (0-0.08 μM) of inhibitor.

## 2.6. Comparison of oil/water partition coefficient assay and ADMET prediction with hit

The physicochemical parameters of a drug are correlated with the membrane permeability of the body. Lipinski's rule of five is used as the rule of thumb when assessing whether a compound can be used as an oral drug [37,38]. For example, the oil/water partition coefficient, which is expressed as a log *P* value, can reflect the absorption of a drug in an organism [39]. The oil/water partition coefficients of

compounds that showed strong potency in bioactivity assessment were measured. As an important parameter, the log $P$ (o/w) (octanol-water partition coefficient) with the optimum central nervous system penetration was around $2.0 \pm 0.7$ [40,41]. Meanwhile, the absorption, distribution, metabolism, excretion, and toxicity (ADMET) properties of the selected five compounds were also predicted by using Discovery Studio Client v18.1.0 [42]. The different descriptors of ADMET characteristics have different prediction levels. Table 5 shows that the log $P$ values of compounds **B9**, **B10**, **B11**, **C4**, and **C6** ranged from 1.78 to 2.42. These results indicate that, according to the hit compound, the modified compounds still retains good lipophilicity (log $P < 5$).   These compounds and the hit compound likely demonstrate good absorption in the human intestine (HIA levels of 0), good solubility in water at 25ºC (solubility levels of 1 and 2) and moderate blood-brain barrier permeability. Moreover, the results show that these compounds are noninhibitors of CYP2D6 (CYP2D6 level of 0) and are highly likely to bind to plasma proteins.

**Table 5.** Log $P$ values and ADMET properties of active compounds.

| Compound | Log P [a] | A [b] | D [c] | | M [d] | E [e] | ALogP98 [f] | PSA2D [g] |
|---|---|---|---|---|---|---|---|---|
| **Hit** | 2.09 | 0 | 2 | 2 | 0 | 1 | 3.06 | 60.14 |
| **B9** | 1.78 | 0 | 2 | 1 | 0 | 1 | 3.891 | 63.493 |
| **B10** | 2.00 | 0 | 1 | 1 | 0 | 1 | 4.24 | 63.493 |
| **B11** | 2.05 | 0 | 1 | 2 | 0 | 1 | 3.352 | 84.308 |
| **C4** | 2.42 | 0 | 1 | 2 | 0 | 1 | 4.016 | 84.308 |
| **C6** | 1.93 | 0 | 1 | 2 | 0 | 1 | 3.557 | 84.308 |

[a] Octanol–water partition coefficients of some compounds were measured by the shake flask method with slight modification.

[b] Absorption: Intestinal absorption.

[c] Distribution: Aqueous solubility and blood-brain barrier penetration.

[d] Metabolism: CYPA2D6.

[e] Excretion: Plasma protein binding.

[f] ALogP98: Predicted octanol/water.

[g] PSA: polar surface area, 2D: two-dimensional.

### 2.7. Cytotoxicity assays and neuroprotective study

To examine the cytotoxicity of the representative compound **C6**, the inherent toxicity towards human hepatoblastoma HepG2 cells and human normal liver cells LO2 were studied using the MTT assay at four different concentrations of compound C6 ranging from 5~50 μM [43]. As shown in Fig. 4A and Fig. 4B, the viability of the modified cells of C6 was almost absent at the concentrations of 10 μM and 25 μM, respectively. With increasing concentrations to 50 μM, C6 decreased cell viability (82.8% and 95.3%, respectively). The results show that the target compound **C6** has a wide range of therapeutic safety for HepG2 cells and LO2 cells. In addition, these preliminary results should encourage further research to explain the neuroprotective mechanisms of compound **C6**.
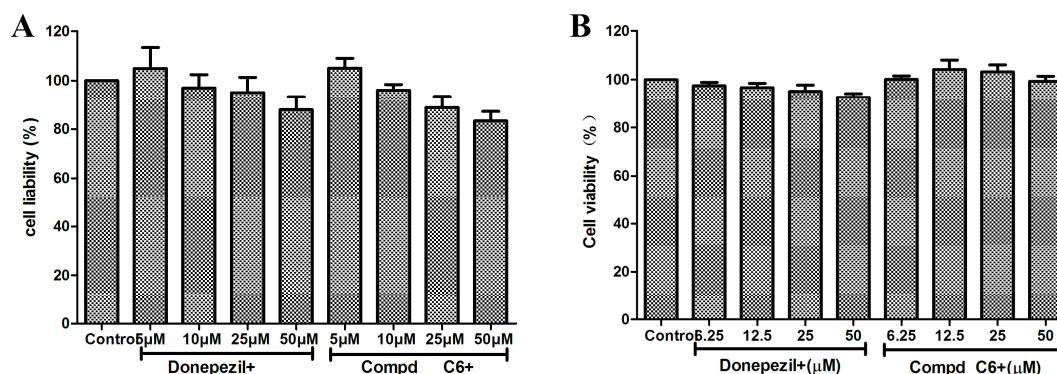


**Fig. 4.** Cytotoxicity of donepezil, compound **C6** tested at concentrations in the range 1–50 μM in HepG2 **(A)** cells and LO2 **(B)** cells for 24 h. Untreated cells were used as control. Results are expressed as percentage of cell survival vs untreated cell (control) and shown as mean ± SD (n = 3)

The protective effects of compound **C6** against free radicals damage were assessed by measuring the ability of the compound to protect against $H_2O_2$ injury according to the reported protocol [44]. After 100 μM $H_2O_2$ exposure, cell viability as determined by

MTT reduction was obviously decreased to 39.8 % ($P < 0.01$ vs control), manifesting high sensitivity to $H_2O_2$-induced injury. However, compound **C6** showed protective effects in a dose-dependent manner against $H_2O_2$-induced PC12 cell injury (Fig. 5). At a concentration of 25 µM, compound **C6** showed neuroprotective effects and was slightly stronger than the positive control donepezil, with a cell viability of 49.6%. When the concentration was reduced to 6.25 µM, the cell viabilities decreased to 40.9%. It clarified that the compound **C6** could capture the hydroxyl radical, generated by $H_2O_2$.
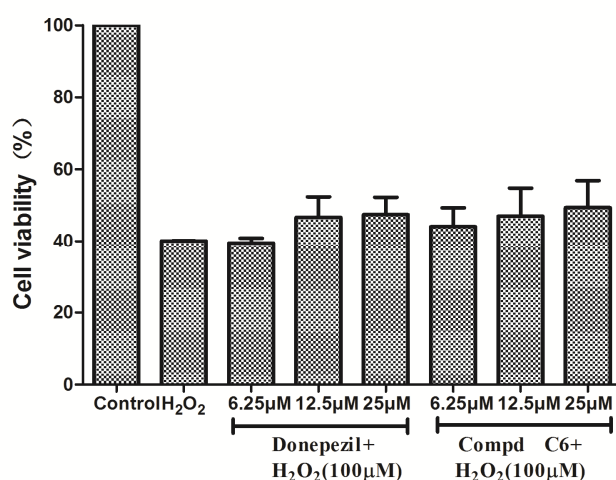


**Fig. 5**. Neuroprotective effect on PC12 neurons of compound **C6**. Results represent mean ± SEM (n = 3). Statistical significance was calculated using one-way ANOVA and Bonferroni post hoc tests. ###$p < 0.001$ compared with the control group; *$p < 0.05$ compared with $H_2O_2$ group; **$p < 0.01$ compared with $H_2O_2$ group; ***$p < 0.001$ compared with $H_2O_2$ group.

## 3. Conclusion

In summary, the structure-based optimization of $\delta$-sulfonolactone-fused pyrazole scaffold was carried out to improve the potency and selectivity of BuChE inhibitors, and 48 compounds were designed and synthesized through the stepwise guidance of structure-activity relationship. By mimicking the hydrophobic interactions of donepezil at PAS, the introduction of a tertiary benzylamine at 5-position can significantly increase BuChE inhibitory activity. Compounds **C4** and **C6** with 4-F/4-Br-substituted

benzylamine at C-5 were identified as high selective nanomolar BuChE inhibitors ($IC_{50}$ = 8.3 and 7.7 nM, respectively). The scavenging ability of compound **C6** has mild values (22.2% for DPPH) comparing to ascorbic acid at a concentration of 100 μM. Kinetic studies indicate that the inhibition of BuChE by compound **C6** is reversible and mixed competitive ($K_i$ = 24 nM). Compound **C6** has been found to be non-toxic to HepG2 cells and LO2 cells, up to 50 μM, with good predictions of ADMET properties, and showing significant neuroprotective activity. Molecular docking showed that compound **C6** was nicely bound to hBuChE *via* a strong hydrogen bond interaction with Asn68, p–π interaction with Leu286, Val288 and Phe329, and a π–anion interaction with His438, Asp70. Compound **C6** has significant potential and can be further developed as a promising therapy for AD treatment.

## 4. Experimental section

### 4.1. Chemistry

#### 4.1.1. General Information

All chemicals, reagents and solvents were purchased from commercial sources and used without further purification. Reactions were checked by thin-layer chromatography (TLC) on precoated silica gel plates (Qingdao Marine Chemical Factory, $GF_{254}$); spots were visualized by UV at 254 nm. Melting points are determined on a XT4MP apparatus (Taike Corp., Beijing, China) and are not corrected. The purity (relative content) of active compounds was determined by HPLC through area normalization method. $^1$H NMR and $^{13}$C NMR spectra were recorded on Bruker AV-300, AV-400 or AV-600 MHz instruments using DMSO-$d_6$ and $CDCl_3$ as solvent. Chemical shifts are reported in parts per million ($\delta$) downfield from the signal of tetramethylsilane (TMS) as internal standards. Coupling constants are reported in Hz. The multiplicity is defined by *s* (singlet), *d* (doublet), *t* (triplet), or *m* (multiplet). High resolution mass spectra (HRMS) were obtained on an Agilent 1260-6221 TOF mass spectrometry.

#### 4.1.2. General procedure for the preparation of compounds *6 (B8) and A1–A14*

To a solution of phenylhydrazine hydrochloride (10.0 mmol) in ethanol (20 mL) was

added saturated NaHCO$_3$ solution (2 mL), acetic acid (5 mL) and ethyl acetoacetate (10.0 mmol), the reaction was heated for 1.5 h at reflux. The mixture was poured into EtOAc (100 mL) and was washed with water and saline solution sequentially, dried over anhydrous MgSO$_4$ for 2 h, filtrated, concentrated to 10 mL, then allowed to stand overnight in cold storage. The mixture was collected by filtration to give the title product **3**.

Ethyl chloroacetoacetate (10.0 mmol) were added to the dioxane (20 mL) solution of phenylhydrazine hydrochloride (10.0 mmol) and the reaction was heated to reflux for 12 h. The mixture was poured into EtOAc (100 mL) and was washed with water and saline solution sequentially, dried over anhydrous MgSO$_4$ for 2 h, filtrated, concentrated to 10 mL, then allowed to stand overnight in refrigeration. The mixture was filtered and collected to get the title product **5**.

To a solution of an oven-dried reaction tube (20 mL) was charged with ethenesulfonyl fluoride (ESF, 0.5 mmol) and the pyrazolone (**3 or 5**, 0.5 mmol, 1.0 equiv), DBU (180 mg dissolved in 10 mL CH$_2$Cl$_2$, 2 mL, 30 mol%), and NaHCO$_3$ (42 mg, 0.5 mmol, 1.0 equiv). The resulting mixture was stirred at room temperature for 12 h with monitoring by TLC. The crude products were purified by column chromatography on silica gel (petroleum ether / EtOAc, 10: 1 to 8: 1) to give the title products **6** and **A1–A14**.

*4.1.2.1 7-(2-fluorophenyl)-5-methyl-4,7-dihydro-3H-[1,2]oxathiino[6,5-c]pyrazole 2,2-dioxide (A1).* Yellow powder, yield 71%; m.p. 132-133ºC; $^1$H NMR (400 MHz, CDCl$_3$) $\delta$ 7.54 – 7.33 (m, 2H), 7.30 – 7.13 (m, 2H), 3.50 (t, $J$ = 6.6 Hz, 2H), 3.12 (t, $J$ = 6.5 Hz, 2H), 2.26 (s, 3H).

*4.1.2.2*

*7-(2-chlorophenyl)-5-cyclopropyl-4,7-dihydro-3H-[1,2]oxathiino[6,5-c]pyrazole 2,2-dioxide (A2).* Light yellow powder, yield 73%; m.p. 112-113ºC; $^1$H NMR (400 MHz, CDCl$_3$) $\delta$ 7.66 (t, $J$ = 2.0 Hz, 1H), 7.52 (dd, $J$ = 8.2, 1.1 Hz, 1H), 7.35 (t, $J$ = 8.1 Hz, 1H), 7.26 (s, 1H), 3.52 (t, $J$ = 6.6 Hz, 2H), 3.21 (t, $J$ = 6.6 Hz, 2H), 1.90 – 1.65 (m, 1H), 1.09 – 0.79 (m, 4H). TOF-HRMS: *m/z* [M + H]$^+$ calcd for C$_{14}$H$_{13}$ClN$_2$O$_3$S: 325.0408; found: 325.0402.

*4.1.2.3  7-(3-chlorophenyl)-5-cyclopropyl-4,7-dihydro-3H-[1,2]oxathiino[6,5-c]pyrazole 2,2-dioxide (**A3**).* Light yellow powder, yield 61%; m.p. 182-183ºC; ^{1}H NMR (400 MHz, CDCl$_3$) $\delta$ 7.50 (t, $J$ = 4.8 Hz, 1H), 7.44 – 7.32 (m, 3H), 3.50 (t, $J$ = 6.5 Hz, 2H), 3.22 (t, $J$ = 6.5 Hz, 2H), 1.85 – 1.72 (m, 1H), 0.98 – 0.89 (m, $J$ = 3.8, 2.2 Hz, 4H). TOF-HRMS: *m/z* [M + H]$^{+}$ calcd for C$_{14}$H$_{13}$ClN$_3$O$_2$S: 325.0408; found: 325.0402.

*4.1.2.4  5-cyclopropyl-7-(2-fluorophenyl)-4,7-dihydro-3H-[1,2]oxathiino[6,5-c]pyrazole 2,2-dioxide (**A4**).* Light yellow powder, yield 81%; m.p. 152-153ºC; ^{1}H NMR (400 MHz, CDCl$_3$) $\delta$ 7.48 – 7.32 (m, $J$ = 8.4, 7.8, 4.2 Hz, 2H), 7.26 – 7.15 (m, $J$ = 10.4, 4.3 Hz, 2H), 3.50 (t, $J$ = 6.5 Hz, 2H), 3.21 (t, $J$ = 6.5 Hz, 2H), 1.85 – 1.70 (m, $J$ = 6.7 Hz, 1H), 1.06 – 0.82 (m, $J$ = 4.0, 2.2 Hz, 4H). TOF-HRMS: *m/z* [M + H]$^{+}$ calcd for C$_{14}$H$_{13}$FN$_2$O$_3$S: 309.0704; found: 309.0704.

*4.1.2.5  5-cyclopropyl-7-(3-fluorophenyl)-4,7-dihydro-3H-[1,2]oxathiino[6,5-c]pyrazole 2,2-dioxide (**A5**).* Light yellow powder, yield 75%; m.p. 122-123ºC; ^{1}H NMR (400 MHz, CDCl$_3$) $\delta$ 7.52 – 7.48 (m, $J$ = 7.8, 1.8 Hz, 1H), 7.44 – 7.29 (m, 3H), 3.50 (t, $J$ = 6.5 Hz, 2H), 3.22 (t, $J$ = 6.5 Hz, 2H), 1.93 – 1.70 (m, 1H), 1.05 – 0.82 (m, 4H). TOF-HRMS: *m/z* [M + H]$^{+}$ calcd for C$_{14}$H$_{13}$FN$_2$O$_3$S: 309.0704; found: 309.0698.

*4.1.2.6  7-(2-fluorophenyl)-5-phenyl-4,7-dihydro-3H-[1,2]oxathiino[6,5-c]pyrazole 2,2-dioxide (**A6**).* Light yellow powder, yield 71%; m.p. 141-142ºC; ^{1}H NMR (400 MHz, CDCl$_3$) $\delta$ 7.73 – 7.66 (m, 2H), 7.60 – 7.51 (m, $J$ = 7.7, 1.7 Hz, 1H), 7.48 – 7.34 (m, 4H), 7.31 – 7.20 (m, 2H), 3.51 (t, $J$ = 6.4 Hz, 2H), 3.38 (t, $J$ = 6.5 Hz, 2H). TOF-HRMS: *m/z* [M + H]$^{+}$ calcd for C$_{17}$H$_{13}$FN$_2$O$_3$S: 345.0704; found: 345.0701.

*4.1.2.7
5-(4-chlorophenyl)-7-(2-fluorophenyl)-4,7-dihydro-3H-[1,2]oxathiino[6,5-c]pyrazole 2,2-dioxide (**A7**).* Light yellow powder, yield 74%; m.p. 105-106ºC; ^{1}H NMR (300 MHz, CDCl$_3$) $\delta$ 7.73 – 7.61 (m, 2H), 7.62 – 7.38 (m, 4H), 7.36 – 7.14 (m, 2H), 3.56 (t, $J$ = 6.4

Hz, 2H), 3.41 (t, $J$ = 6.3 Hz, 2H). TOF-HRMS: $m/z$ [M + H]$^+$ calcd for $C_{17}H_{12}ClFN_2O_3S$: 379.0314; found: 379.0314.

*4.1.2.8*

*5-(4-bromophenyl)-7-(2-fluorophenyl)-4,7-dihydro-3H-[1,2]oxathiino[6,5-c]pyrazole 2,2-dioxide (A8).* Light yellow powder, yield 82%; m.p. 136-137ºC; $^1$H NMR (300 MHz, CDCl$_3$) $\delta$ 7.65 – 7.41 (m, 6H), 7.39 – 7.23 (m, 2H), 3.56 (t, $J$ = 6.4 Hz, 2H), 3.41 (t, $J$ = 6.5 Hz, 2H). TOF-HRMS: $m/z$ [M + H]$^+$ calcd for $C_{17}H_{12}BrFN_2O_3S$: 422.9809; found: 422.9808.

*4.1.2.9*

*7-(2-fluorophenyl)-5-(4-fluorophenyl)-4,7-dihydro-3H-[1,2]oxathiino[6,5-c]pyrazole 2,2-dioxide (A9).* Yellow powder, yield 91%; m.p. 142-145ºC; $^1$H NMR (400 MHz, CDCl$_3$) $\delta$ 7.73 – 7.66 (m, 2H), 7.58 – 7.52 (m, 1H), 7.49 – 7.42 (m, 1H), 7.29 (t, $J$ = 7.7 Hz, 2H), 7.14 (t, $J$ = 8.7 Hz, 2H), 3.55 (t, $J$ = 6.4 Hz, 2H), 3.40 (t, $J$ = 6.4 Hz, 2H). $^{13}$C NMR (101 MHz, CDCl$_3$) $\delta$ 163.18, 156.31, 148.56, 146.05, 131.03, 128.78, 128.69(2C), 128.16, 125.03, 124.29, 117.12, 116.08(2C), 93.85, 44.87, 20.08. TOF-HRMS: $m/z$ [M + H]$^+$ calcd for $C_{17}H_{12}F_2N2O_3S$: 363.0609; found: 363.0604.

*4.1.2.10    7-(2-chlorophenyl)-5-phenyl-4,7-dihydro-3H-[1,2]oxathiino[6,5-c]pyrazole 2,2-dioxide (A10).* Yellow powder, yield 78%; m.p. 104-106ºC; $^1$H NMR (400 MHz, CDCl3) $\delta$ 7.73 (d, $J$ = 7.1 Hz, 2H), 7.54 (ddd, $J$ = 14.6, 7.4, 2.0 Hz, 2H), 7.48 – 7.37 (m, 5H), 3.54 (t, $J$ = 6.3 Hz, 2H), 3.44 (t, $J$ = 6.2 Hz, 2H). $^{13}$C NMR (101 MHz, CDCl3) $\delta$ 149.02, 146.12, 134.04, 132.52, 132.00, 131.14, 130.71, 129.64 (2C), 129.01, 128.85, 127.86, 126.92 (2C), 93.64, 45.00, 20.18. TOF-HRMS: $m/z$ [M + H]$^+$ calcd for $C_{17}H_{13}ClN_2O_3S$: 361.0408; found: 361.0402.

*4.1.2.11*

*7-(2-chlorophenyl)-5-(4-chlorophenyl)-4,7-dihydro-3H-[1,2]oxathiino[6,5-c]pyrazole 2,2-dioxide (A11).* Yellow powder, yield 83%; m.p. 172-173ºC; $^1$H NMR (400 MHz, CDCl$_3$) $\delta$ 7.70 – 7.63 (m, 2H), 7.56 (dd, $J$ = 7.8, 1.7 Hz, 1H), 7.53 – 7.37 (m, 5H), 3.55 (t,

$J$ = 6.4 Hz, 2H), 3.43 (t, $J$ = 6.4 Hz, 2H). TOF-HRMS: $m/z$ [M + H]$^+$ calcd for C$_{17}$H$_{12}$Cl$_2$N2O$_3$S: 395.0018; found: 395.0019.

*4.1.2.12*

*5-(4-bromophenyl)-7-(2-chlorophenyl)-4,7-dihydro-3H-[1,2]oxathiino[6,5-c]pyrazole 2,2-dioxide (A12).* Yellow Powder, yield 68%; m.p. 110-112ºC; $^1$H NMR (400 MHz, CDCl$_3$) $\delta$ 7.66 – 7.53 (m, 5H), 7.53 – 7.38 (m, 3H), 3.55 (t, $J$ = 6.5 Hz, 2H), 3.42 (t, $J$ = 6.4 Hz, 2H). TOF-HRMS: $m/z$ [M + H]$^+$ calcd for C$_{17}$H$_{12}$BrClN$_2$O$_3$S: 438.9513; found: 438.9508.

*4.1.2.13*

*7-(2-chlorophenyl)-5-(4-fluorophenyl)-4,7-dihydro-3H-[1,2]oxathiino[6,5-c]pyrazole 2,2-dioxide (A13).* Light yellow powder, yield 81%; m.p. 141-143ºC; $^1$H NMR (400 MHz, CDCl$_3$) $\delta$ 7.75 – 7.64 (m, 2H), 7.56 (dd, $J$ = 7.8, 1.6 Hz, 1H), 7.51 (dd, $J$ = 7.4, 2.1 Hz, 1H), 7.44 (td, $J$ = 7.4, 1.9 Hz, 2H), 7.14 (t, $J$ = 8.7 Hz, 2H), 3.55 (t, $J$ = 6.5 Hz, 2H), 3.42 (t, $J$ = 6.4 Hz, 2H). TOF-HRMS: $m/z$ [M + H]$^+$ calcd for C$_{17}$H$_{12}$ClFN$_2$O$_3$S: 379.0314; found: 379.0313.

*4.1.2.14*

*7-(4-chlorophenyl)-5-(4-methoxyphenyl)-4,7-dihydro-3H-[1,2]oxathiino[6,5-c]pyrazole 2,2-dioxide (A14).* Light yellow powder, yield 61%; m.p. 92-95ºC; $^1$H NMR (600 MHz, CDCl$_3$) $\delta$ 7.78 – 7.57 (m, 4H), 7.48 – 7.41 (m, 2H), 7.03 – 6.95 (m, 2H), 3.86 (s, 3H), 3.55 (t, $J$ = 6.5 Hz, 2H), 3.40 (t, $J$ = 6.5 Hz, 2H). TOF-HRMS: $m/z$ [M + H]$^+$ calcd for C$_{18}$H$_{15}$ClN$_2$O$_4$S: 391.0514; found: 391.0507.

*4.1.3. General procedure for the preparation of compounds* **B1–B14**

To a solution of compound **6** (1 mmol) in MeCN (20 mL) was added the secondary amine (**HNR$_2$R$_3$**, 1.2 equiv) and K$_2$CO$_3$ (1.2 equiv). The suspension solution was stirred at room temperature for 12 h, and subjected to column chromatography on silica gel (CH$_2$Cl$_2$ / methanol, 50: 1) to obtain the title products **B1–B14**.

*4.1.3.1*

*5-(chloromethyl)-7-(2-chlorophenyl)-4,7-dihydro-3H-[1,2]oxathiino[6,5-c]pyrazole 2,2-dioxide (**B1**).* Yellow powder, yield 51%; m.p. 192-195ºC; $^1$H NMR (400 MHz, CDCl$_3$) $\delta$ 7.56 – 7.52 (m, 1H), 7.47 – 7.37 (m, 3H), 4.60 (s, 2H), 3.53 (t, $J$ = 6.6 Hz, 2H), 3.30 (t, $J$ = 6.5 Hz, 2H). TOF-HRMS: *m/z* [M + H]$^+$ calcd for C$_{12}$H$_{10}$Cl$_2$N$_2$O$_3$S: 332.9862; found: 332.9863.

*4.1.3.2*

*5-((benzyl(methyl)amino)methyl)-7-(2-chlorophenyl)-4,7-dihydro-3H-[1,2]oxathiino[6,5-c]pyrazole 2,2-dioxide (**B2**).* Colorless oil, yield 51%; $^1$H NMR (600 MHz, CDCl$_3$) $\delta$ 7.52 (d, $J$ = 8.1 Hz, 1H), 7.43 – 7.26 (m, 8H), 3.57 (s, 2H), 3.55 (s, 2H), 3.46 (t, $J$ = 6.6 Hz, 2H), 3.21 (t, $J$ = 6.5 Hz, 2H), 2.26 (s, 3H). $^{13}$C NMR (101 MHz, CDCl$_3$) $\delta$ 148.41, 145.84, 138.76, 133.96, 132.11, 131.01, 130.64, 129.51 (2C), 129.38 (2C), 128.53, 127.77, 127.49, 95.12, 62.40, 54.59, 45.17, 42.65, 18.69. TOF-HRMS: *m/z* [M + H]$^+$ calcd for C$_{20}$H$_{20}$ClN$_3$O$_3$S: 418.0987; found: 418.0992.

*4.1.3.3*

*5-((benzyl(ethyl)amino)methyl)-7-(2-chlorophenyl)-4,7-dihydro-3H-[1,2]oxathiino[6,5-c] pyrazole 2,2-dioxide (**B3**).* Colorless oil, yield 53%; $^1$H NMR (400 MHz, CDCl$_3$) $\delta$ 7.52 (dd, $J$ = 5.1, 4.5 Hz, 1H), 7.45 – 7.36 (m, 3H), 7.36 – 7.26 (m, 5H), 3.73 – 3.65 (m, $J$ = 10.7, 6.3 Hz, 6H), 3.43 (t, $J$ = 6.5 Hz, 2H), 3.06 (t, $J$ = 6.5 Hz, 2H), 2.78 (t, $J$ = 5.3 Hz, 2H). $^{13}$C NMR (101 MHz, CDCl$_3$) $\delta$ 147.82, 145.67, 138.22, 133.65, 131.83, 130.90, 130.51, 129.29 (2C), 129.27 (2C), 128.48, 127.63, 127.48, 94.76, 58.99, 58.70, 55.84, 50.89, 44.80, 18.32. TOF-HRMS: *m/z* [M + H]$^+$ calcd for C$_{21}$H$_{22}$ClN$_3$O$_4$S: 448.1092; found: 448.1089.

*4.1.3.4*

*5-((benzyl(2-hydroxyethyl)amino)methyl)-7-(2-chlorophenyl)-4,7-dihydro-3H-[1,2]oxathiino[6,5-c]pyrazole 2,2-dioxide (**B4**).* Colorless oil, yield 68%; $^1$H NMR (400 MHz, CDCl$_3$) $\delta$ 7.51 (d, $J$ = 7.9 Hz, 1H), 7.45 – 7.32 (m, 6H), 7.26 (s, 2H), 3.60 (s, 4H), 3.43 (t,

$J$ = 6.4 Hz, 2H), 3.19 (t, $J$ = 6.3 Hz, 2H), 2.58 (d, $J$ = 6.7 Hz, 2H), 1.11 (t, $J$ = 6.9 Hz, 3H). TOF-HRMS: $m/z$ [M + H]$^+$ calcd for $C_{21}H_{22}ClN_3O_3S$: 432.1143; found: 432.1145.

*4.1.3.5*

*7-(2-chlorophenyl)-5-(morpholinomethyl)-4,7-dihydro-3H-[1,2]oxathiino[6,5-c]pyrazole 2,2-dioxide (**B5**).* Colorless oil, yield 63%; $^1$H NMR (400 MHz, CDCl$_3$) $\delta$ 7.55 – 7.49 (m, 1H), 7.45 – 7.34 (m, 3H), 3.76 – 3.69 (m, 4H), 3.55 (s, 2H), 3.50 (t, $J$ = 6.5 Hz, 2H), 3.27 (t, $J$ = 6.5 Hz, 2H), 2.51 (s, 4H). TOF-HRMS: $m/z$ [M + H]$^+$ calcd for $C_{16}H_{18}FN_3O_3S$: 384.0779; found: 384.0778.

*4.1.3.6*

*7-(2-chlorophenyl)-5-((4-methylpiperazin-1-yl)methyl)-4,7-dihydro-3H-[1,2]oxathiino[6, 5-c]pyrazole 2,2-dioxide (**B6**).* Colorless oil, yield 55%; $^1$H NMR (400 MHz, CDCl$_3$) $\delta$ 7.52 (d, $J$ = 7.8 Hz, 1H), 7.47 – 7.32 (m, 3H), 3.57 (s, 2H), 3.48 (t, $J$ = 6.5 Hz, 2H), 3.26 (t, $J$ = 6.4 Hz, 2H), 2.52 (d, $J$ = 28.1 Hz, 8H), 2.30 (s, $J$ = 13.3 Hz, 3H). $^{13}$C NMR (101 MHz, CDCl$_3$) $\delta$ 147.70, 145.74, 133.92, 131.98, 131.00, 130.60, 129.49, 127.75, 95.07, 55.66, 55.17 (2C), 52.86 (2C), 45.92, 45.12, 18.78. TOF-HRMS: $m/z$ [M + H]$^+$ calcd for $C_{17}H_{21}ClN_4O_3S$: 397.1096; found: 397.1092.

*4.1.3.7*

*5-((4-benzylpiperazin-1-yl)methyl)-7-(2-chlorophenyl)-4,7-dihydro-3H-[1,2]oxathiino[6, 5-c]pyrazole 2,2-dioxide (**B7**).* Colorless oil, yield 54%; $^1$H NMR (400 MHz, CDCl$_3$) $\delta$ 7.51 (d, $J$ = 7.7 Hz, 1H), 7.46 – 7.34 (m, $J$ = 16.8, 7.4 Hz, 3H), 7.34 – 7.27 (m, $J$ = 14.5, 4.0 Hz, 5H), 3.55 (d, $J$ = 15.1 Hz, 4H), 3.48 (t, $J$ = 6.5 Hz, 2H), 3.26 (t, $J$ = 6.5 Hz, 2H), 2.53 (s, 8H). $^{13}$C NMR (101 MHz, CDCl$_3$) $\delta$ 147.51, 145.55, 137.44, 133.74, 131.82, 130.81, 130.42, 129.34 (2C), 129.31 (2C), 128.27, 127.56, 127.23, 94.95, 62.89, 55.49, 52.93(2C), 52.87(2C), 44.94, 18.61. TOF-HRMS: $m/z$ [M + H]$^+$ calcd for $C_{23}H_{25}ClN_4O_3S$: 473.1409; found: 473.1409.

*4.1.3.8*

*5-(chloromethyl)-7-(2-fluorophenyl)-4,7-dihydro-3H-[1,2]oxathiino[6,5-c]pyrazole*

*2,2-dioxide (**B8**).* Yellow powder, yield 61%; m.p. 162-163ºC; ^{1}H NMR (400 MHz, CDCl$_3$) *δ* 7.53 – 7.40 (m, 2H), 7.29 (d, *J* = 7.2 Hz, 1H), 7.24 (d, *J* = 9.0 Hz, 1H), 4.61 (s, 2H), 3.55 (t, *J* = 6.6 Hz, 2H), 3.31 (t, *J* = 6.6 Hz, 2H). TOF-HRMS: *m/z* [M + H]$^+$ calcd for C$_{12}$H$_{10}$ClFN$_2$O$_3$S: 317.0157; found: 317.0158.

### 4.1.3.9

*5-((benzyl(methyl)amino)methyl)-7-(2-fluorophenyl)-4,7-dihydro-3H-[1,2]oxathiino[6,5-c]pyrazole 2,2-dioxide (**B9**).* Light yellow oil, yield 66%; ^{1}H NMR (400 MHz, CDCl$_3$) *δ* 7.49 – 7.36 (m, 2H), 7.32 (s, 5H), 7.25 – 7.18 (m, 2H), 3.57 (s, 2H), 3.55 (s, 2H), 3.46 (t, *J* = 6.4 Hz, 2H), 3.20 (t, *J* = 6.3 Hz, 2H), 2.26 (s, 3H). ^{13}C NMR (101 MHz, CDCl$_3$) *δ* 156.06, 148.92, 145.47, 138.79, 130.52, 129.13, 128.33 (2C), 127.81 (2C), 127.25, 124.72, 124.19, 116.87, 95.25, 62.38, 54.66, 44.93, 42.64, 18.53. TOF-HRMS: *m/z* [M + H]$^+$ calcd for C$_{20}$H$_{20}$FN$_3$O$_3$S: 402.1282; found: 402.1284.

### 4.1.3.10

*5-((benzyl(ethyl)amino)methyl)-7-(2-fluorophenyl)-4,7-dihydro-3H-[1,2]oxathiino[6,5-c] pyrazole 2,2-dioxide (**B10**).* Light yellow oil, yield 71%; ^{1}H NMR (400 MHz, CDCl$_3$) *δ* 7.48 – 7.34 (m, 3H), 7.31 (d, *J* = 3.5 Hz, 4H), 7.25 – 7.19 (m, 2H), 3.60 (s, 4H), 3.42 (t, *J* = 6.4 Hz, 2H), 3.17 (t, *J* = 6.4 Hz, 2H), 2.59 (dd, *J* = 13.5, 6.6 Hz, 2H), 1.12 (t, *J* = 6.9 Hz, 3H). ^{13}C NMR (101 MHz, CDCl$_3$) *δ* 156.20, 149.52, 145.55, 130.60, 129.25 (2C), 128.72, 128.37 (2C), 127.95, 127.16, 124.86, 124.36, 117.02, 95.42, 58.43, 51.56, 48.15, 45.05, 18.72, 12.10. TOF-HRMS: *m/z* [M + H]$^+$ calcd for C$_{21}$H$_{22}$FN$_3$O$_3$S: 416.1439; found: 416.1442.

### 4.1.3.11

*5-((benzyl(2-hydroxyethyl)amino)methyl)-7-(2-fluorophenyl)-4,7-dihydro-3H-[1,2]oxathiino[6,5-c]pyrazole 2,2-dioxide (**B11**).* Colorless oil, yield 73%; ^{1}H NMR (400 MHz, CDCl$_3$) *δ* 7.51 – 7.38 (m, 2H), 7.37 – 7.26 (m, 6H), 7.23 (d, *J* = 9.6 Hz, 1H), 3.68 (m, 6H), 3.42 (t, *J* = 6.5 Hz, 2H), 3.05 (t, *J* = 6.5 Hz, 2H), 2.78 (t, *J* = 5.3 Hz, 2H). ^{13}C NMR (101 MHz, CDCl$_3$) *δ* 156.18, 148.57, 145.65, 138.54, 130.78, 129.39 (2C), 128.64 (2C),

127.92, 127.60, 124.95, 124.26, 117.10, 95.23, 59.26, 59.00, 56.13, 51.30, 44.90, 18.49. TOF-HRMS: $m/z$ [M + H]$^+$ calcd for $C_{21}H_{22}FN_3O_4S$: 432.1388; found: 432.1392.

4.1.3.12

*7-(2-fluorophenyl)-5-(morpholinomethyl)-4,7-dihydro-3H-[1,2]oxathiino[6,5-c]pyrazole 2,2-dioxide (**B12**).* Colorless oil, yield 58%; $^1$H NMR (400 MHz, CDCl$_3$) $\delta$ 7.48 (dd, $J$ = 7.1, 1.5 Hz, 2H), 7.30 – 7.26 (m, 2H), 3.76 (t, $J$ = 5.7, 4.3 Hz, 4H), 3.61 (s, 2H), 3.54 (t, $J$ = 6.5 Hz, 2H), 3.31 (t, $J$ = 6.5 Hz, 2H), 2.58 (s, 4H). $^{13}$C NMR (101 MHz, CDCl$_3$) $\delta$ 156.02, 147.57, 145.48, 130.64, 127.80, 124.76, 124.09, 116.87, 95.36, 66.94 (2C), 56.05, 53.60 (2C), 44.87, 18.58. TOF-HRMS: $m/z$ [M + H]$^+$ calcd for $C_{16}H_{18}FN_3O_4S$: 368.1075; found: 368.1080.

4.1.3.13

*7-(2-fluorophenyl)-5-((4-methylpiperazin-1-yl)methyl)-4,7-dihydro-3H-[1,2]oxathiino[6, 5-c]pyrazole 2,2-dioxide (**B13**).* Colorless oil, yield 61%; $^1$H NMR (400 MHz, CDCl$_3$) $\delta$ 7.46 – 7.37 (m, 2H), 7.20 (dd, $J$ = 16.9, 8.1 Hz, 2H), 3.55 (s, 2H), 3.48 (t, $J$ = 6.5 Hz, 2H), 3.21 (t, $J$ = 6.5 Hz, 2H), 2.60 (s, 8H), 2.37 (s, 3H). $^{13}$C NMR (101 MHz, CDCl$_3$) $\delta$ 156.20, 147.87, 145.62, 130.80, 128.01, 124.92, 124.29, 117.05, 95.53, 55.42, 54.94 (2C), 52.34 (2C), 45.51, 45.06, 19.36. TOF-HRMS: $m/z$ [M + H]$^+$ calcd for $C_{17}H_{21}FN_4O_3S$: 381.1391; found: 381.1392.

4.1.3.14

*5-((4-benzylpiperazin-1-yl)methyl)-7-(2-fluorophenyl)-4,7-dihydro-3H-[1,2]oxathiino[6, 5-c]pyrazole 2,2-dioxide (**B14**).* Colorless oil, yield 58%; $^1$H NMR (400 MHz, CDCl$_3$) $\delta$ 7.48 – 7.37 (m, 2H), 7.35 – 7.30 (m, 5H), 7.25 – 7.19 (m, 2H), 3.58 (s, 2H), 3.56 (s, 2H), 3.49 (t, $J$ = 6.5 Hz, 2H), 3.25 (t, $J$ = 6.5 Hz, 2H), 2.57 (s, 8H). $^{13}$C NMR (101 MHz, CDCl$_3$) $\delta$ 156.18, 148.11, 145.58, 130.73, 129.55 (2C), 128.56, 128.49 (2C), 127.99, 127.46, 124.89, 124.31, 117.02, 95.54, 63.06, 55.69, 53.09 (4C), 45.07, 18.82. TOF-HRMS: $m/z$ [M + H]$^+$ calcd for $C_{23}H_{25}FN_4O_3S$: 457.1704; found: 457.1701.

*4.1.4. General procedure for the preparation of compounds **C1–C10***

K$_2$CO$_3$ (1.2 equiv) was added to a solution of compound **6** (1 mmol, 1.2 equiv) and the hydroxyethyl benzylamine (HNR$^2$R$^3$, 1 mmol) in MeCN (20 mL), then the reaction mixture was stirred at room temperature for 12 h, and subjected to column chromatography on silica gel (CH$_2$Cl$_2$ / methanol, 50: 1) to obtain the title products **C1–C10** .

*4.1.4.1*

*5-(((3-fluorobenzyl)(2-hydroxyethyl)amino)methyl)-7-(2-fluorophenyl)-4,7-dihydro-3H-[ 1,2]oxathiino[6,5-c]pyrazole 2,2-dioxide (**C1**).* Light yellow oil, yield 69%; purity, 99.8%. $^1$H NMR (400 MHz, CDCl$_3$) $\delta$ 7.51 – 7.37 (m, *J* = 14.0, 6.4 Hz, 2H), 7.32 – 7.24 (m, 3H), 7.08 (t, 2H), 6.96 (t, *J* = 7.4 Hz, 1H), 3.71 (d, *J* = 13.2 Hz, 6H), 3.45 (d, *J* = 6.2 Hz, 2H), 3.11 (t, *J* = 6.1 Hz, 2H), 2.81–2.73 (m, 2H). TOF-HRMS: *m/z* [M + H]+ calcd for C$_{21}$H$_{21}$F$_2$N$_3$O$_4$S: 450.1294; found: 450.1296.

*4.1.4.2*

*5-(((3-chlorobenzyl)(2-hydroxyethyl)amino)methyl)-7-(2-fluorophenyl)-4,7-dihydro-3H-[ 1,2]oxathiino[6,5-c]pyrazole 2,2-dioxide (**C2**).* Light yellow oil, yield 66%; purity, 99.9%. $^1$H NMR (400 MHz, CDCl$_3$) $\delta$ 7.51 – 7.39 (m, 2H), 7.33 (s, 1H), 7.29 – 7.18 (m, 5H), 3.70 (s, 2H), 3.68 (s, 2H), 3.67 (s, 2H), 3.45 (t, *J* = 6.5 Hz, 2H), 3.09 (t, *J* = 6.5 Hz, 2H), 2.78 (t, *J* = 5.2 Hz, 2H). $^{13}$C NMR (101 MHz, CDCl$_3$) $\delta$ 156.13, 148.34, 145.66, 140.85, 134.38, 130.81, 129.90, 129.25, 127.86, 127.69, 127.40, 124.95, 124.18, 117.08, 95.19, 59.43, 58.56, 56.32, 51.23, 44.87, 18.52. TOF-HRMS: *m/z* [M + H]$^+$ calcd for C$_{21}$H$_{21}$ClFN$_3$O$_4$S: 466.0998; found: 466.0997.

*4.1.4.3*

*5-(((3-bromobenzyl)(2-hydroxyethyl)amino)methyl)-7-(2-fluorophenyl)-4,7-dihydro-3H-[ 1,2]oxathiino[6,5-c]pyrazole 2,2-dioxide (**C3**).* Light yellow oil, yield 70%; purity, 99.2%. $^1$H NMR (400 MHz, CDCl$_3$) $\delta$ 7.51 – 7.37 (m, 5H), 7.28 (s, 1H), 7.24 – 7.16 (m, 3H), 3.69 (s, 2H), 3.67 (s, 2H), 3.66 (s, 2H), 3.46 (t, *J* = 6.5 Hz, 2H), 3.08 (t, *J* = 6.5 Hz,

2H), 2.79 (t, $J$ = 5.3 Hz, 2H). $^{13}$C NMR (101 MHz, CDCl$_3$) $\delta$ 156.18, 148.41, 145.70, 141.26, 132.21, 130.83, 130.65, 130.24, 127.91, 127.89, 124.97, 124.23, 122.69, 117.12, 95.18, 59.49, 58.57, 56.40, 51.24, 44.92, 18.59. TOF-HRMS: $m/z$ [M + H]$^+$ calcd for C$_{21}$H$_{21}$BrFN$_3$O$_4$S: 510.0493; found: 510.0489.

*4.1.4.4*

*5-(((4-fluorobenzyl)(2-hydroxyethyl)amino)methyl)-7-(2-fluorophenyl)-4,7-dihydro-3H-[ 1,2]oxathiino[6,5-c]pyrazole 2,2-dioxide (**C4**).* Light yellow oil, yield 53%; purity, 99.5%. $^1$H NMR (400 MHz, CDCl$_3$) $\delta$ 7.51 – 7.41 (m, 2H), 7.32 – 7.25 (m, 4H), 7.03 (t, $J$ = 8.1 Hz, 2H), 3.70 (s, 2H), 3.68 (s, 4H), 3.47 (t, $J$ = 6.2 Hz, 2H), 3.10 (t, $J$ = 6.2 Hz, 2H), 2.78 (s, 2H). $^{13}$C NMR (101 MHz, CDCl$_3$) $\delta$ 162.28, 156.18, 148.49, 145.68, 134.21, 130.89 (2C), 130.79, 127.88, 124.96, 124.21, 117.11, 115.46 (2C), 95.15, 59.30, 58.14, 55.96, 51.03, 44.88, 18.53. TOF-HRMS: $m/z$ [M + H]$^+$ calcd for C$_{21}$H$_{21}$F$_2$N$_3$O$_4$S: 450.1294; found: 450.1294.

*4.1.4.5*

*5-(((4-chlorobenzyl)(2-hydroxyethyl)amino)methyl)-7-(2-fluorophenyl)-4,7-dihydro-3H-[ 1,2]oxathiino[6,5-c]pyrazole 2,2-dioxide (**C5**).* Light yellow oil, yield 58%; purity, 99.7%. $^1$H NMR (400 MHz, CDCl$_3$) $\delta$ 7.55 – 7.38 (m, 3H), 7.32 – 7.27 (m, 3H), 7.25 – 7.21 (m, 2H), 3.68 (s, 2H), 3.66 (s, 4H), 3.45 (t, $J$ = 6.5 Hz, 2H), 3.08 (t, $J$ = 6.5 Hz, 2H), 2.76 (t, $J$ = 5.3 Hz, 2H). $^{13}$C NMR (101 MHz, CDCl$_3$) $\delta$ 156.00, 148.28, 145.51, 136.93, 133.13, 130.68, 130.48 (2C), 128.60 (2C), 127.72, 124.81, 124.04, 116.95, 94.99, 59.20, 58.11, 55.93, 50.94, 44.72, 18.38. TOF-HRMS: $m/z$ [M + H]$^+$ calcd for C$_{21}$H$_{21}$ClFN$_3$O$_4$S: 466.0998; found: 466.0999.

*4.1.4.6*

*5-(((4-bromobenzyl)(2-hydroxyethyl)amino)methyl)-7-(2-fluorophenyl)-4,7-dihydro-3H-[ 1,2]oxathiino[6,5-c]pyrazole 2,2-dioxide (**C6**).* Light yellow oil, yield 61%; purity,

99.7%. $^1$H NMR (400 MHz, CDCl$_3$) $\delta$ 7.52 – 7.40 (m, 4H), 7.28 (d, $J$ = 7.8 Hz, 2H), 7.22 (dd, $J$ = 8.9, 4.7 Hz, 2H), 3.73 – 3.62 (m, $J$ = 4.2 Hz, 6H), 3.47 (t, $J$ = 6.5 Hz, 2H), 3.10 (t, $J$ = 6.5 Hz, 2H), 2.77 (t, $J$ = 5.3 Hz, 2H). $^{13}$C NMR (101 MHz, CDCl$_3$) $\delta$ 156.17, 148.45, 145.68, 137.67, 131.72 (2C), 130.99 (2C), 130.84, 127.88, 124.97, 124.20, 121.39, 117.12, 95.12, 59.38, 58.34, 56.13, 51.12, 44.88, 18.55. TOF-HRMS: $m/z$ [M + H]$^+$ calcd for C$_{21}$H$_{21}$BrFN$_3$O$_4$S: 510.0493; found: 510.0493.

### 4.1.4.7

*5-(((2,4-dichlorobenzyl)(2-hydroxyethyl)amino)methyl)-7-(2-fluorophenyl)-4,7-dihydro-3 H-[1,2]oxathiino[6,5-c]pyrazole 2,2-dioxide (**C7**).* Light yellow oil, yield 83%; purity, 95.7%. $^1$H NMR (400 MHz, CDCl$_3$) $\delta$ 7.47 – 7.34 (m, 4H), 7.26 – 7.16 (m, 3H), 3.79 (s, 2H), 3.67 (s, 2H), 3.65 (s, 2H), 3.43 (t, $J$ = 6.4 Hz, 2H), 3.07 (t, $J$ = 6.4 Hz, 2H), 2.77 (s, 2H). $^{13}$C NMR (101 MHz, CDCl$_3$) $\delta$ 155.99, 147.96, 145.51, 135.04, 134.55, 133.92, 132.49, 130.68, 129.56, 127.70, 127.14, 124.80, 124.02, 116.94, 95.17, 59.17, 56.20, 55.93, 47.66, 44.72, 18.25. TOF-HRMS: $m/z$ [M + H]$^+$ calcd for C$_{21}$H$_{20}$Cl$_2$FN$_3$O$_4$S: 500.0608; found: 500.0606.

### 4.1.4.8

*7-(2-fluorophenyl)-5-(((2-hydroxyethyl)(4-methylbenzyl)amino)methyl)-4,7-dihydro-3H-[ 1,2]oxathiino[6,5-c]pyrazole 2,2-dioxide (**C8**).* Light yellow oil, yield 69%; purity, 98.5%. $^1$H NMR (400 MHz, CDCl$_3$) $\delta$ 7.51 – 7.36 (m, 2H), 7.25 (dd, $J$ = 10.2, 6.3 Hz, 2H), 7.19 (d, $J$ = 7.9 Hz, 2H), 7.12 (d, $J$ = 7.8 Hz, 2H), 3.65 (d, $J$ = 9.6 Hz, 6H), 3.43 (t, $J$ = 6.5 Hz, 2H), 3.07 (t, $J$ = 6.5 Hz, 2H), 2.76 (t, $J$ = 4.9 Hz, 2H), 2.33 (s, 3H). $^{13}$C NMR (101 MHz, CDCl$_3$) $\delta$ 156.14, 148.61, 145.63, 137.22, 135.31, 131.10, 130.73, 129.33 (2C), 129.28 (2C), 127.89, 124.92, 124.25, 117.05, 95.24, 59.19, 58.64, 55.95, 51.26, 44.89, 21.28, 18.50. TOF-HRMS: $m/z$ [M + H]$^+$ calcd for C$_{22}$H$_{24}$FN$_3$O$_4$S: 446.1544; found: 446.1547.

### 4.1.4.9

*7-(2-fluorophenyl)-5-(((2-hydroxyethyl)(4-methoxybenzyl)amino)methyl)-4,7-dihydro-3H*

*-[1,2]oxathiino[6,5-c]pyrazole 2,2-dioxide (C9).* Light yellow oil, yield 53%; purity, 95.7%. $^1$H NMR (400 MHz, CDCl$_3$) $\delta$ 7.52 – 7.36 (m, 2H), 7.29 – 7.19 (m, 4H), 6.86 (d, $J$ = 7.7 Hz, 2H), 3.79 (s, 3H), 3.66 (s, 4H), 3.64 (s, 2H), 3.44 (t, $J$ = 6.2 Hz, 2H), 3.07 (t, $J$ = 6.2 Hz, 2H), 2.76 (t, 2H). $^{13}$C NMR (101 MHz, CDCl$_3$) $\delta$ 159.08, 156.17, 148.69, 145.64, 140.90, 136.82, 130.75, 130.57 (2C), 127.91, 124.93, 124.26, 117.07, 113.96 (2C), 95.20, 59.20, 58.25, 55.88, 55.44, 51.12, 44.91, 18.53. TOF-HRMS: *m/z* [M + H]$^+$ calcd for C$_{22}$H$_{24}$FN$_3$O$_5$S: 462.1493; found: 462.1488.

### 4.1.4.10

*5-(((3,4-dimethoxybenzyl)(2-hydroxyethyl)amino)methyl)-7-(2-fluorophenyl)-4,7-dihydro -3H-[1,2]oxathiino[6,5-c]pyrazole 2,2-dioxide (C10).* Light yellow oil, yield 62%; purity, 99.8%. $^1$H NMR (400 MHz, CDCl$_3$) $\delta$ 7.52 – 7.38 (m, 2H), 7.29 (d, $J$ = 5.7 Hz, 1H), 7.23 (d, $J$ = 9.9 Hz, 1H), 6.92 (s, 1H), 6.83 (q, $J$ = 8.2 Hz, 2H), 3.87 (s, 3H), 3.84 (s, 3H), 3.68 (d, $J$ = 7.9 Hz, 6H), 3.46 (t, $J$ = 6.4 Hz, 2H), 3.10 (t, $J$ = 6.4 Hz, 2H), 2.78 (s, 2H). $^{13}$C NMR (101 MHz, CDCl$_3$) $\delta$ 156.00, 148.96, 148.53, 148.35, 145.53, 130.74, 130.66, 127.74, 124.86, 124.12, 121.47, 116.96, 112.47, 110.98, 95.14, 59.15, 58.47, 55.96, 55.94, 55.84, 50.70, 44.76, 18.45. TOF-HRMS: *m/z* [M + H]$^+$ calcd for C$_{23}$H$_{26}$FN$_3$O$_6$S: 492.1599; found: 492.1598.

### 4.1.5. General procedure for the preparation of compounds D1–D10

K$_2$CO$_3$ (1.2 equiv) was added to a solution of compound 6 (1 mmol, 1.2 equiv) and the secondary amine (HNR$^2$R$^3$, 1 mmol) in MeCN (20 mL), then the reaction mixture was stirred at room temperature for 12 h, and subjected to column chromatography on silica gel (CH2Cl2 / methanol, 50: 1) to obtain the title products **D1–D10.**

### 4.1.5.1

*5-((benzyl(2-methoxyethyl)amino)methyl)-7-(2-fluorophenyl)-4,7-dihydro-3H-[1,2]oxathi ino[6,5-c]pyrazole 2,2-dioxide (D1).* Light yellow oil, yield 63%; $^1$H NMR (400 MHz, CDCl$_3$) $\delta$ 7.42 (dt, $J$ = 12.9, 7.4 Hz, 2H), 7.34 – 7.28 (m, 4H), 7.26 – 7.16 (m, 3H), 3.68 (s, 4H), 3.52 (t, $J$ = 5.1 Hz, 2H), 3.43 (t, $J$ = 6.4 Hz, 2H), 3.30 (s, 3H), 3.21 (t, $J$ = 6.4 Hz, 2H), 2.74 (t, $J$ = 4.6 Hz, 2H). $^{13}$C NMR (101 MHz, CDCl$_3$) $\delta$ 156.20, 149.44, 145.58,

139.35, 130.65, 130.61, 128.39 (2C), 127.93 (2C), 127.26, 124.86, 124.36, 117.02, 95.59, 71.42, 59.66, 58.79, 53.49, 52.55, 45.10, 18.61. TOF-HRMS: m/z [M + H]+ calcd for $C_{22}H_{24}FN_3O_4S$: 446.1544; found: 446.1545.

*4.1.5.2*

*5-(((4-fluorobenzyl)(2-methoxyethyl)amino)methyl)-7-(2-fluorophenyl)-4,7-dihydro-3H-[1,2]oxathiino[6,5-c]pyrazole 2,2-dioxide (**D2**).* Light yellow oil, yield 61%; ^{1}H NMR (400 MHz, CDCl$_3$) δ 7.47 – 7.36 (m, 2H), 7.31 – 7.25 (m, 3H), 7.23 – 7.18 (m, 1H), 6.99 (t, *J* = 8.2 Hz, 2H), 3.65 (s, 2H), 3.63 (s, 2H), 3.50 (s, 2H), 3.45 (t, *J* = 6.4 Hz, 2H), 3.30 (s, 3H), 3.20 (t, *J* = 6.3 Hz, 2H), 2.70 (s, 2H). ^{13}C NMR (101 MHz, CDCl$_3$) δ 161.95, 156.03, 149.10, 145.45, 134.78, 130.53 (3C), 127.74, 124.70, 124.14, 116.87, 115.02 (2C), 95.33, 71.22, 58.63, 58.57, 53.10, 52.14, 44.91, 18.46. TOF-HRMS: *m/z* [M + H]$^+$ calcd for $C_{22}H_{23}F_2N_3O_4S$: 464.1450; found: 464.1454.

*4.1.5.3*

*5-(((4-chlorobenzyl)(2-methoxyethyl)amino)methyl)-7-(2-fluorophenyl)-4,7-dihydro-3H-[1,2]oxathiino[6,5-c]pyrazole 2,2-dioxide (**D3**).* Light yellow oil, yield 65%; ^{1}H NMR (400 MHz, CDCl$_3$) δ 7.51 – 7.41 (m, 2H), 7.34 – 7.25 (m, 6H), 3.70 (s, 2H), 3.68 (s, 2H), 3.55 (t, *J* = 5.1 Hz, 2H), 3.49 (t, *J* = 6.5 Hz, 2H), 3.34 (s, 3H), 3.24 (t, *J* = 6.5 Hz, 2H), 2.75 (t, J = 4.9 Hz, 2H). ^{13}C NMR (101 MHz, CDCl$_3$) δ 156.02, 149.00, 145.45, 137.66, 132.75, 130.50, 130.38, 128.35 (2C), 127.73 (2C), 124.70, 124.12, 116.86, 95.33, 71.20, 58.64 (2C), 53.17, 52.19, 44.89, 18.46. TOF-HRMS: *m/z* [M + H]$^+$ calcd for $C_{22}H_{23}ClFN_3O_4S$: 480.1155; found: 480.1156.

*4.1.5.4*

*5-(((4-bromobenzyl)(2-methoxyethyl)amino)methyl)-7-(2-fluorophenyl)-4,7-dihydro-3H-[1,2]oxathiino[6,5-c]pyrazole 2,2-dioxide (**D4**).* Light yellow oil, yield 65%; ^{1}H NMR (400 MHz, CDCl$_3$) δ 7.47 – 7.36 (m, 4H), 7.25 – 7.16 (m, 4H), 3.66 (s, 2H), 3.62 (s, 2H), 3.50 (t, *J* = 5.1 Hz, 2H), 3.45 (t, *J* = 6.5 Hz, 2H), 3.31 (d, *J* = 8.0 Hz, 3H), 3.20 (t, *J* = 6.4 Hz, 2H), 2.71 (t, *J* = 5.0 Hz, 2H). ^{13}C NMR (101 MHz, CDCl$_3$) δ 156.21, 149.16, 145.64,

138.39, 131.49 (2C), 130.94 (2C), 130.69, 127.92, 124.89, 124.31, 121.02, 117.05, 95.51, 58.88, 58.83, 53.38, 52.40, 45.08, 18.65. TOF-HRMS: *m/z* [M + H]$^+$ calcd for C$_{22}$H$_{23}$BrFN$_3$O$_4$S: 524.0649; found: 524.0650.

*4.1.5.5*

*5-((ethyl(4-fluorobenzyl)amino)methyl)-7-(2-fluorophenyl)-4,7-dihydro-3H-[1,2]oxathiin o[6,5-c]pyrazole 2,2-dioxide (**D5**).* Light yellow oil, yield 63%; $^1$H NMR (400 MHz, CDCl$_3$) $\delta$ 7.39 (m, 2H), 7.21 (m, 4H), 6.97 (t, *J* = 8.4 Hz, 2H), 3.56 (s, 2H), 3.54 (s, 2H), 3.42 (t, *J* = 6.5 Hz, 2H), 3.15 (t, *J* = 6.4 Hz, 2H), 2.54 (d, *J* = 6.5 Hz, 2H), 1.08 (t, *J* = 6.8 Hz, 3H). $^{13}$C NMR (101 MHz, CDCl$_3$) $\delta$ 160.71, 156.02, 149.17, 145.42, 134.91, 130.57, 130.48 (2C), 127.74, 124.70, 124.14, 116.86, 115.01 (2C), 95.19, 57.35, 51.10, 47.76, 44.85, 18.57, 11.86. TOF-HRMS: *m/z* [M + H]$^+$ calcd for C$_{21}$H$_{21}$F$_2$N$_3$O$_3$S: 434.1344; found: 434.1344.

*4.1.5.6*

*5-(((4-chlorobenzyl)(ethyl)amino)methyl)-7-(2-fluorophenyl)-4,7-dihydro-3H-[1,2]oxathi ino[6,5-c]pyrazole 2,2-dioxide (**D6**).* Light yellow oil, yield 67%; $^1$H NMR (400 MHz, CDCl$_3$) $\delta$ 7.45 – 7.33 (m, 2H), 7.24 – 7.18 (m, 6H), 3.56 (s, 2H), 3.54 (s, 2H), 3.43 (t, *J* = 6.4 Hz, 2H), 3.15 (t, *J* = 6.2 Hz, 2H), 2.53 (s, 2H), 1.08 (t, *J* = 6.0 Hz, 3H). $^{13}$C NMR (101 MHz, CDCl$_3$) $\delta$ 156.23, 149.33, 145.64, 132.91, 131.13, 130.71, 130.56, 128.56 (2C), 127.95 (2C), 124.91, 124.33, 117.08, 95.37, 57.65, 51.48, 48.07, 45.05, 18.80, 12.09. TOF-HRMS: *m/z* [M + H]$^+$ calcd for C$_{21}$H$_{21}$ClFN$_3$O$_3$S: 450.1049; found: 450.1050.

*4.1.5.7*

*5-(((4-bromobenzyl)(ethyl)amino)methyl)-7-(2-fluorophenyl)-4,7-dihydro-3H-[1,2]oxathi ino[6,5-c]pyrazole 2,2-dioxide (**D7**).* Light yellow oil, yield 60%; $^1$H NMR (400 MHz, CDCl$_3$) $\delta$ 7.50 – 7.38 (m, 5H), 7.25 – 7.17 (m, 4H), 3.56 (s, 4H), 3.46 (t, *J* = 6.5 Hz, 2H), 3.18 (t, *J* = 6.6 Hz, 2H), 2.59 (s, 2H), 1.12 (t, *J* = 6.7 Hz, 3H). $^{13}$C NMR (101 MHz, CDCl$_3$) $\delta$ 156.19, 149.18, 145.60, 131.74, 131.47 (2C), 130.89 (2C), 130.68, 128.74, 127.92, 124.89, 124.29, 117.04, 95.35, 57.70, 51.39, 48.06, 45.01, 18.76, 12.07. TOF-HRMS: *m/z* [M + H]$^+$ calcd for C$_{21}$H$_{21}$BrFN$_3$O$_3$S: 494.0544; found: 494.0546.

*4.1.5.8*

*5-(((4-fluorobenzyl)(methyl)amino)methyl)-7-(2-fluorophenyl)-4,7-dihydro-3H-[1,2]oxat hiino[6,5-c]pyrazole 2,2-dioxide (**D8**).* Light yellow oil, yield 62%; $^1$H NMR (400 MHz, CDCl$_3$) $\delta$ 7.51 – 7.37 (m, 2H), 7.27 – 7.30 (m, 2H), 7.26 – 7.19 (m, 2H), 7.01 (t, $J$ = 8.6 Hz, 2H), 3.54 (s, 4H), 3.49 (t, $J$ = 6.5 Hz, 2H), 3.20 (t, $J$ = 6.5 Hz, 2H), 2.24 (s, 3H). $^{13}$C NMR (101 MHz, CDCl$_3$) $\delta$ 162.06, 156.06, 148.72, 145.49, 134.37, 130.60 (2C), 130.57, 127.80, 124.74, 124.15, 116.89, 115.14(2C), 95.21, 61.45, 54.52, 44.90, 42.45, 18.55. TOF-HRMS: *m/z* [M + H]$^+$ calcd for C$_{20}$H$_{19}$F$_2$N$_3$O$_3$S: 420.1188; found: 420.1187.

*4.1.5.9*

*5-(((4-chlorobenzyl)(methyl)amino)methyl)-7-(2-fluorophenyl)-4,7-dihydro-3H-[1,2]oxat hiino[6,5-c]pyrazole 2,2-dioxide (**D9**).* Light yellow oil, yield 59%; $^1$H NMR (400 MHz, CDCl$_3$) $\delta$ 7.61 – 7.36 (m, 3H), 7.36 – 7.27 (m, 3H), 7.26 – 7.18 (m, 2H), 3.54 (s, 4H), 3.48 (t, $J$ = 6.3 Hz, 2H), 3.20 (t, $J$ = 5.2 Hz, 2H), 2.23 (s, 3H). $^{13}$C NMR (101 MHz, CDCl$_3$) $\delta$ 156.04, 148.65, 145.50, 137.25, 132.90, 130.59, 130.41 (2C), 128.47 (2C), 127.80, 124.76, 124.14, 116.89, 95.25, 61.47, 54.62, 44.88, 42.50, 18.56. TOF-HRMS: *m/z* [M + H]$^+$ calcd for C$_{20}$H$_{19}$ClFN$_3$O$_3$S: 436.0892; found: 436.0891.

*4.1.5.10*

*5-(((4-bromobenzyl)(methyl)amino)methyl)-7-(2-fluorophenyl)-4,7-dihydro-3H-[1,2]oxat hiino[6,5-c]pyrazole 2,2-dioxide (**D10**).* Light yellow oil, yield 60%; $^1$H NMR (400 MHz, CDCl$_3$) $\delta$ 7.51 – 7.33 (m, 4H), 7.26 – 7.19 (m, 4H), 3.59 – 3.41 (m, 6H), 3.20 (t, $J$ = 6.4 Hz, 2H), 2.23 (s, 3H). $^{13}$C NMR (101 MHz, CDCl$_3$) $\delta$ 156.05, 148.67, 145.50, 137.82, 131.43 (2C), 130.75 (2C), 130.58, 127.79, 124.75, 124.14, 121.00, 116.89, 95.21, 61.54, 54.67, 44.89, 42.54, 18.57. TOF-HRMS: *m/z* [M + H]$^+$ calcd for C$_{20}$H$_{19}$BrFN$_3$O$_3$S: 480.0387; found: 480.0387.

## 4.2. EeAChE and eqBuChE inhibition assays

Assays were performed on AChE from electric eel (C3389-500UN; Sigma) and BuChE from equine serum (C4290-1KU; Sigma), according to the Ellman's method. The experiment was performed in 48-well plates in a final volume of 500 µL. Each well contained 0.036 U/mL of EeAChE or eqBuChE, and 0.1 M pH 8 phosphate buffer. They were preincubated for 20 min at different compound concentrations at 37 ºC. Then 0.35 mM acetylthiocholine iodide (ACh; A5751-1G; Sigma) or 0.5 mM butyrylthiocholine iodide (BuCh; 20820-1G; Sigma) and 0.35 mM 5,5'-ditiobis-2-nitrobenzoico (DTNB; D8130-1G; Sigma) were added. The DTNB produces the yellow anion 5-thio-2-nitrobenzoic acid along with the enzymatic degradation of ACh or BuCh. Changes in absorbance were measured at 410 nm after 20 min in a Biotek Synergy HTX Multi-Mode reader. The $IC_{50}$ values were determined graphically from inhibition curves (log inhibitor concentration *vs* percent of inhibition). A control experiment was performed under the same conditions without inhibitor and the blank contained buffer, DMSO, DTNB, and substrate.

## 4.3. Radical scavenging activity (DPPH assay)

The antioxidant capacity of the test compounds were evaluated by DPPH method in which DPPH free radical chould be scavenged by antioxidant. Briefly, 150 mL of the compound (100 µM) with 150 mL of DPPH (140 µM) was mixed and incubated in a 96-well plate for 2 h in the dark at 37ºC. The relevant absorbance of the reaction mixture was measured at 520 nm using a microplate reader (BioTek Synergy HT). The reducing percentage (RP) of DPPH was determined by the formula: $RP = (1 - A_C/A_0) \times 100\%$, where $Ac/A_0$ are DPPH absorbance in the presence and absence of inhibitors, respectively. Ascorbic acid was used as a standard for DPPH determination.

## 4.4. Oil/water partition coefficient assay and ADMET prediction

Using the classical shake flask method, the oil/water partition coefficient of the compounds were tested. The same amount of oleic phase (noctanol) and aqueous phase

(PBS pH 7.4) were mixed. And the mixture was shaken by ultrasonic (400 W, 40 kHz) and allowed to stand for 24 h to obtain a saturated solution of noctanol. An appropriate amount of the compounds was added. After sealing, the test compounds was shaken at 37ºC for 48 h to make it fully equilibrated in the two phases. Then the mixture was measured with a high performance liquid chromatography.

The active compounds were analyzed with the ADMET prediction tools of Discovery Studio Client v18.1.0. The pharmacokinetic properties are HIA (human intestinal absorption), PPB (plasma protein binding), Cytochrome P450 2D6 binding (CYP2D6), Aqueous solubility, and BBB. ADMET screening in a stepwise manner is summarized as follows. HIA: there are four prediction levels of 0–3 represent good, moderate, low, and very low absorption respectively. The data displayed that eleven compounds had good absorption (HIA levels of 0, score < 6.126), one compounds had moderate absorption and one had low absorption. Aqueous solubility: solubility levels of 0–5 represent extremely low; no, very low, but possible; yes, low; yes, good; yes, optimal; no, too soluble respectively, and we found these compounds show at least possible solubility (solubility level of 1 and 2). BBB: BBB levels of 0–4 represent very high, high, medium, low, and undefined penetration. The results showed that nine compounds had high penetrant, there compounds had medium penetrant and two compounds had undefined penetration. CYP2D6 binding activity: CYP2D6 is involved in the metabolism of a wide range of substrates in the liver and its inhibition by a drug constitutes a major of drug-drug interaction. The level of 0 and 1 reflect as non-inhibitor and inhibitor. The results showed that active compounds were non-inhibitors of CYP2D6 (CYP2D6 level of 0). PPB: PPB levels of 0 and1 reflect on binding as < 90%, binding as > 90%.

### 4.5. Kinetic studies of eqBuChE inhibition.

Kinetic studies were performed with the same test conditions, using six concentrations of substrate (0.1-1 mM) and four concentrations of inhibitor (0-0.08 μM). Apparent inhibition constants and kinetic parameters were calculated within the "Enzyme kinetics" module of Prism 5. The effect of concentrations of compound **C6** on the activity for the catalysis of BuChE at 37ºC was also studied. Assay conditions were same as described in assay protocol except that the final concentration of enzyme was varied (0-0.72 U/mL).

Concentrations of compound **C6** (0, 0.02, 0.04, 0.08μM) were used respectively, for the determination of reversible as well as irreversible binding of inhibitors at enzyme.

### 4.6. Molecular docking study

A structure based in silico procedure was applied to discover the binding modes of the active compounds to BuChE enzyme active site. The CDOCKER of Discovery Studio Client v18.1.0 (DS) was conducted to explain SAR of series compounds and further guide the design of more effective and concrete BuChE inhibitors. The ligand binding to the crystal structure of $h$BuChE with PDB ID: 5LKR was selected as template. The target enzyme was prepared with Prepare Protein of DS to ensure the integrity of target. The ligand was processed by Full Minimization of the Small Molecular in DS. Then title compounds were docked into the active site of protein using CDOCKER. The view results of molecular docking were extracted after the program running end, each docking result was analyzed for interaction and their different pose. Those poses with the lowest -CDOCKER_INTERACTION_ENERGY values were regarded as the most stable and picked to analysis binding interactions with target enzyme visualized.

### 4.7. Cytotoxicity assays

Human hepatoblastoma cells HepG2 and human normal liver cells LO2 were maintained at 37°C in a humidified incubator containing 5% $CO_2$ in DMEM containing 10% fetal bovine serum, 100 U/mL penicillin, and 100 μg/mL streptomycin. Cell cytotoxicity was evaluated by methyl thiazolyl tetrazolium (MTT) assay. HepG2 cells and LO2 cells were inoculated at $1 \times 104$ cells per well in 96-well plate. After cultured for 24 h, the cells were treated with different compounds which were diluted in DMEM for 24 h. Then 20 μL of 0.5 mg/mL MTT reagent was added into the cells and incubated for 4 h. After 4 h, cell culture was removed and then 150 μL DMSO was added to dissolve the formazan. The optical density was measured at 492 nm (OD492). Cell viability was calculated from three independent experiments. The density of formazan formed in blank group was set as 100% of viability. Cell viability (%) = compound (OD492 / blank (OD492) $\times$ 100%

Blank: cultured with fresh medium only.

Compound: treated with compounds or donepezil.

## 4.8. Neuroprotection assay

PC12 cells were dispensed into 96-well microtiter plates at a density of $1 \times 10^4$ cells/well. Following incubation overnight, cells were treated with a range of compound C6 concentrations (1–25 μM) at time zero and maintained for 3 h. Then, the media were replaced by fresh media still containing the drug plus the cytotoxic stimulus represented by 100 μM $H_2O_2$ that was left for an additional 24 h period. Cell viability was measured after 24 h by using the MTT assay. Briefly, 20 µL of 0.5 mg/mL MTT reagent was added into the cells and incubated for 4 h. After 4 h, cell culture was removed and then 150 µL DMSO was added to dissolve the formazan. The optical density was measured at 492 nm (OD492) on the Biotek Synergy HTX Multi-Mode reader. Results were adjusted considering OD measured in the blank.

## 4.9. Statistical analysis

Data are reported as mean ± SEM of at least three independent experiments and data analysis was performed with GraphPad Prism 6 software.

## Acknowledgments

## Notes

The authors declare no competing financial interest.

## Abbreviations used

ACh, acetylcholine; BuChE, butyrylcholinesterase; AChE, acetylcholinesterase; AD,

Alzheimer's disease; SuFEx, sulfur (VI) fluoride exchange; ADMET, absorption, distribution, metabolism, excretion and toxicity in pharmacokinetics; ChE, cholinesterase; PD, Parkinson disease; EeAChE, *Electrophorus electricus* AChE; eqBuChE, equine BuChE; AChEIs, AChE inhibitors; BBB, blood-brain barrier; HIA, human intestinal absorption; PPB, plasma protein binding; CYP2D6, Cytochrome P450 2D6.

**Appendix A. Supplementary material**

The copies of representative $^1$H and $^{13}$C NMR spectra can be found at http://

**References**

[1] Alzheimer's Association, Alzheimer's disease facts and figures, Alzheimers Dement. 14 (2018) 367-425.

[2] P. Scheltens, K. Blennow, M.M.B. Breteler, B. de Strooper, G.B. Frisoni, S. Salloway, W.M. Van der Flier, Alzheimer's disease, Lancet 388(10043) (2016) 505-517.

[3] A.K. Ghosh, H.L. Osswald, BACE1 (beta-secretase) inhibitors for the treatment of Alzheimer's disease, Chem. Soc. Rev. 43 (2014) 6765-6813.

[4] M. Rosini, E. Simoni, A. Milelli, A. Minarini, C. Melchiorre, Oxidative Stress in Alzheimer's Disease: Are We Connecting the Dots? J. Med. Chem. 57(7) (2014) 2821-2831.

[5] R.M. Anderson, C. Hadjichrysanthou, S. Evans, M.M. Wong, Why do so many clinical trials of therapies for Alzheimer's disease fail? Lancet 390(10110) (2017) 2327-2329.

[6] S.Y. Hung, W.M. Fu, Drug candidates in clinical trials for Alzheimer's disease, J. Biomed. Sci. 24 (2017) 47.

[7] P. Zhang, S. Xu, Z. Zhu, J. Xu, Multi-target design strategies for the improved treatment of Alzheimer's disease. Eur. J. Med. Chem. 176 (2019) 228-247.

[8] R.S. Kumar, A.I. Almansour, N. Arumugam, D.M. Al-Thamili, A. Basiri, D. Kotresha, T.S. Manohar, S. Venketesh, M. Asad, A.M. Asiri, Highly functionalized 2-amino-4H-pyrans as potent cholinesterase inhibitors, Bioorg. Med. Chem. 81 (2018) 134-143.

[9] T.H. Ferreira-Vieira, I.M. Guimaraes, F.R. Silva, F.M. Ribeiro, Alzheimer's disease: targeting the cholinergic system, Curr. Neuropharmacol. 14 (2016) 101-115.

[10] Q. Li, S. He, Y. Chen, F. Feng, W. Qu, H. Sun, Donepezil-based multi-functional cholinesterase inhibitors for treatment of Alzheimer's disease, Eur. J. Med. Chem. 158 (2018) 463-477.

[11] X. Norel, M. Angrisani, C. Labat, I. Gorenne, E. Dulmet, F. Rossi, C. Brink, Degradation of acetylcholine in human airways: role of butyrylcholinesterase, Br. J. Pharmacol. 108(4) (1993) 914-919.

[12] A. Contestabile, The history of the cholinergic hypothesis, Behav. Brain Res. 221 (2011) 334-340.

[13] N.H. Greig, T. Utsuki, D.K. Ingram, Y. Wang, G. Pepeu, C. Scali, Q.-S. Yu, J. Mamczarz, H.W. Holloway, T. Giordano, D.M. Chen, K. Furukawa, K. Sambamurti, A. Brossi, D.K. Lahiri, Selective butyrylcholinesterase inhibition elevates brain acetylcholine, augments learning and lowers Alzheimer beta-amyloid peptide in rodent, Proc. Natl. Acad. Sci. U.S.A. 102 (2005) 17213-17218.

[14] N. Kandiah, M.-C. Pai, V. Senanarong, I. Looi, E. Ampil, K.W. Park, A.K. Karanam, S. Christopher, Rivastigmine: the advantages of dual inhibition of acetylcholinesterase and butyrylcholinesterase and its role in subcortical vascular dementia and Parkinson's disease dementia, Clin. Interv. Aging 12 (2017) 697-707.

[15] G.A. Reid, S. Darvesh, Butyrylcholinesterase-knockout reduces brain deposition of fibrillar β-amyloid in an Alzheimer mouse model, Neuroscience 298 (2015) 424-435.

[16] T. Maurice, M. Strehaiano, N. Simeon, C. Bertrand, A. Chatonnet, Learning performances and vulnerability to amyloid toxicity in the butyrylcholinesterase knockout mouse, Behav. Brain Res. 296 (2016) 351-360.

[17] S. Darvesh, G.A. Reid, Reduced fibrillar beta-amyloid in subcortical structures in a butyrylcholinesterase-knockout Alzheimer disease mouse model, Chem.-Biol. Interact. 259 (2016) 307-312.

[18] D.R. DeBay, G.A. Reid, I.R. Macdonald, G. Mawko, S. Burrell, E. Martin, C.V. Bowen, S. Darvesh, Butyrylcholinesterase-knockout reduces fibrillar beta-amyloid and conserves (18)FDG retention in 5XFAD mouse model of Alzheimer's disease, Brain Res. 1671 (2017) 102-110.

[19] A. Saxena, A.M. Redman, X. Jiang, O. Lockridge, B.P. Doctor, Differences in active site gorge dimensions of cholinesterases revealed by binding of inhibitors to human butyrylcholinesterase, Biochemistry 36 (1997) 14642-14651.

[20] Y. Nicolet, O. Lockridge, P. Masson, J.C. Fontecilla-Camps, F. Nachon, Crystal structure of human butyrylcholinesterase and of its complexes with substrate and products. J. Biol. Chem. 278 (2003) 41141-41147.

[21] V. Cavallaro, Y.F. Moglie, A.P. Murray, G.E. Radivoy, Alkynyl and beta-ketophosphonates: Selective and potent butyrylcholinesterase inhibitors, Bioorg. Chem. 77 (2018) 420-428.

[22] S.-C. Chen, G.-L. Qiu, B. Li, J.-B. Shi, X.-H. Liu, W.-J. Tang, Tricyclic pyrazolo[1,5-d][1,4] benzoxazepin-5(6H)-one scaffold derivatives: Synthesis and biological evaluation as selective BuChE inhibitors, Eur. J. Med. Chem. 147 (2018) 194-204.

[23] T.P.C. Chierrito, S. Pedersoli-Mantoani, C. Roca, V. Sebastian-Perez, L. Martinez-Gonzalez, D.I. Perez, C. Perez, A. Canales, F. Javier Canada, N.E. Campillo, I. Carvalho, A. Martinez, Chameleon-like behavior of indolylpiperidines in complex with cholinesterases targets: Potent butyrylcholinesterase inhibitors, Eur. J. Med. Chem. 145 (2018) 431-444.

[24] U. Kosak, B. Brus, D. Knez, S. Zakelj, J. Trontelj, A. Pislar, R. Sink, M. Jukic, M. Zivin, A. Podkowa, F. Nachon, X. Brazzolotto, J. Stojan, J. Kos, N. Coquelle, K. Salat, J.-P. Colletier, S. Gobec, The magic of crystal structure-based inhibitor optimization: Development of a butyrylcholinesterase inhibitor with picomolar affinity and in vivo activity, J. Med. Chem. 61(1) (2018) 119-139.

[25] L. Jing, G. Wu, D. Kang, Z. Zhou, Y. Song, X. Liu, P. Zhan, Contemporary medicinal-chemistry strategies for the discovery of selective butyrylcholinesterase inhibitors, Drug Discov Today, S1359-6446 (2018) 30333-7.

[26] J. Mo, T. Chen, H. Yang, Y. Guo, Q. Li, Y. Qiao, H. Lin, F. Feng, W. Liu, Y. Chen, Z. Liu, H. Sun, Design, synthesis, in vitro and in vivo evaluation of benzylpiperidine-linked 1,3-dimethylbenzimidazolinones as cholinesterase inhibitors against Alzheimer's disease, J. Enzyme Inhib. Med. Chem. 35 (2020) 330-343.

[27] J. Dong, L. Krasnova, M.G. Finn, K.B. Sharpless, Sulfur(VI) fluoride exchange

(SuFEx): Another good reaction for click chemistry, Angew. Chem.-Int. Edit. 53 (2014) 9430-9448.

[28]  X. Chen, G.-F. Zha, W.-Y. Fang, K.P. Rakesh, H.-L. Qin, A portal to a class of novel sultone-functionalized pyridines via an annulative SuFEx process employing earth abundant nickel catalysts, Chem. Commun. 54 (2018) 9011-9014.

[29]  S. Mondal, Recent developments in the synthesis and application of sultones, Chem. Rev. 112 (2012) 5339-5355.

[30]  H.-W. Xu, L.-J. Zhao, H.-F. Liu, D. Zhao, J. Luo, X.-P. Xie, W.-S. Liu, J.-X. Zheng, G.-F. Dai, H.-M. Liu, L.-H. Liu, Y.-B. Liang, Synthesis and anti-BVDV activity of novel delta-sultones in vitro: Implications for HCV therapies, Bioorg. Med. Chem. Lett. 24 (2014) 2388-2391.

[31]  C. Zhao, K.P. Rakesh, L. Ravidar, W.Y. Fang, H.L. Qin, Pharmaceutical and medicinal significance of sulfur (SVI)-Containing motifs for drug discovery: A critical review, Eur. J. Med. Chem. 162 (2019) 679-734.

[32]  X. Chen, G.-F. Zha, G.A.L. Bare, J. Leng, S.-M. Wang, H.-L. Qin, Synthesis of a class of fused delta-sultone heterocycles via DBU-catalyzed direct annulative SuFEx click of ethenesulfonyl fluorides and pyrazolones or 1,3-dicarbonyl compounds, Adv. Synth. Catal. 359 (2017) 3254-3260.

[33]  Y. Xu, Z. Zhang, X. Jiang, X. Chen, Z. Wang, H. Alsulami, H.L. Qin, W. Tang, Discovery of δ-sultone-fused pyrazoles for treating Alzheimer's disease: Design, synthesis, biological evaluation and SAR studies, Eur. J. Med. Chem. 181 (2019) 111598.

[34]  R. Farina, L. Pisani, M. Catto, O. Nicolotti, D. Gadaleta, N. Denora, R. Soto-Otero, E. Mendez-Alvarez, C.S. Passos, G. Muncipinto, C.D. Altomare, A. Nurisso, P.A. Carrupt, A. Carotti, Structure-Based Design and Optimization of Multitarget-Directed 2H-Chromen-2-one Derivatives as Potent Inhibitors of Monoamine Oxidase B and Cholinesterases, J. Med. Chem. 58 (2015) 5561-5578.

[35]  M. Zhang, Z. Wang, Y. Zhang, W. Guo, H. Ji, Structure-Based Optimization of Small-Molecule Inhibitors for the β-Catenin/B-Cell Lymphoma 9 Protein-Protein Interaction, J. Med. Chem. 61 (2018) 2989-3007.

[36]  S.N. Dighe, G.S. Deora, E. De la Mora, F. Nachon, S. Chan, M.O. Parat, X.

Brazzolotto, B.P. Ross, Discovery and Structure–Activity Relationships of a Highly Selective Butyrylcholinesterase Inhibitor by Structure-Based Virtual Screening, J. Med. Chem. 59 (2016) 7683-7689.

[37] L. Di, E.H. Kerns, I.F. Bezar, S.L. Petusky, Y. Huang, Comparison of blood-brain barrier permeability assays: in situ brain perfusion, MDR1-MDCKII and PAMPA-BBB, J. Pharm. Sci. 98 (2009) 1980-1991.

[38] P.A. Nogara, A. Saraiva Rde, D. Caeran Bueno, L.J. Lissner, C. Lenz Dalla Corte, M.M. Braga, D.B. Rosemberg, J.B. Rocha, Virtual screening of acetylcholinesterase inhibitors using the Lipinski's rule of five and ZINC databank, BioMed Res. Int. 2015 (2015) 870389.

[39] D.G. Levitt, Quantitative relationship between the octanol/water partition coefficient and the diffusion limitation of the exchange between adipose and blood, BMC Clin. Pharmacol. 10 (2010) 1.

[40] W.J. Tang, J. Wang, X. Tong, J.B. Shi, X.H. Liu, J. Li, Design and synthesis of celastrol derivatives as anticancer agents, Eur. J. Med. Chem. 95 (2015) 166-173.

[41] V. Thiyagarajan, S.H. Lin, Y.C. Chang, C.F. Weng, Identification of novel FAK and S6K1 dual inhibitors from natural compounds via ADMET screening and molecular docking, Biomed. Pharmacother. 80 (2016) 52-62.

[42] J. Grover, V. Kumar, V. Singh, K. Bairwa, M.E. Sobhia, S.M. Jachak, Synthesis, biological evaluation, molecular docking and theoretical evaluation of ADMET properties of nepodin and chrysophanol derivatives as potential cyclooxygenase (COX-1, COX-2) inhibitors, Eur. J. Med. Chem. 80 (2014) 47-56.

[43] S.N. Dighe, G.S. Deora, E. De la Mora, F. Nachon, S. Chan, M.-O. Parat, X. Brazzolotto, B.P. Ross, Discovery and structure-activity relationships of a highly selective butyrylcholinesterase inhibitor by structure-based virtual screening, J. Med. Chem. 59(16) (2016) 7683-7689.

[44] Y. Li, X. Qiang, L. Luo, X. Yang, G. Xiao, Q. Liu, J. Ai, Z. Tan, Y. Deng. Aurone Mannich base derivatives as promising multifunctional agents with acetylcholinesterase inhibition, anti-β-amyloid aggragation and neuroprotective properties for the treatment of Alzheimer's disease. Eur. J. Med. Chem. 126 (2016) 762-775.

- Optimization improved BuChE inhibition of $\delta$-Sultone-fused pyrazoles.

- Introduction of a tertiary benzylamine increased BuChE inhibition.

- $IC_{50}$ values of **C4** and **C6** are 8.3 and 7.7 nM, respectively.

- **C6** showed mild antioxidant capacity (22.2% for DPPH).

- **C6** exhibited neuroprotective activity.

**Declaration of interests**

✓  ☐ The authors declare that they have no known competing financial interests or personal relationships that could have appeared to influence the work reported in this paper.

☐ The authors declare the following financial interests/personal relationships which may be considered as potential competing interests:

The authors declare that they have no conflict of interets.